DESTRUCTION OF VOLATILE ORGANIC COMPOUNDS IN A DIELECTRIC BARRIER DISCHARGE PLASMA REACTOR

By

VIJAY KALPATHI

Bachelor of Technology

Indian Institute of Technology Madras,

Chennai, India

2002

Submitted to the faculty of the
Graduate College of
Oklahoma State University
In partial fulfillment of
The requirements for
The Degree of
MASTER OF SCIENCE
May, 2005

DESTRUCTION OF VOLATILE ORGANIC COMPOUNDS IN A DIELECTRIC BARRIER DISCHARGE PLASMA REACTOR

Thesis Approved:

Arland H. Johannes
Thesis Advisor

Gary L. Foutch

John N. Veenstra

A. Gordon Emslie

Dean of the Graduate College

ACKNOWLEDGMENTS

I would like to thank my academic advisor Dr. A.H. Johannes for his guidance and inspiration during the research. I would also like to thank my committee members Dr. Gary Foutch, and Dr. John Veenstra for their time and support.

A special note of thanks goes to Dr. Greg Holland, who was a constant source of motivation, help and encouragement throughout the research.

I wish to thank the staff and graduate students of the School of Chemical Engineering for all their help and assistance. I am also thankful to the School of Chemical Engineering for financial support.

I would like to express special gratitude to Rajbharath Paneerselvam for his active participation in conducting experiments with me and making them more interesting, and Visalakshi Annamalai and for her help in setting up the electrical circuit in the laboratory.

I am indebted to my parents whose blessings have carried my so far, and I want to thank my wife Sarah, who has provided ceaseless encouragement and support when I needed it most.

TABLE OF CONTENTS

LIST OF TABLES

LIST OF FIGURES

NOMENCLATURE

τ Residence Time (s)

E Electric Field (V/cm)

n Neutral Gas Density (cm^{-3})

E/n Reduced Electric Field (Townsend)

Td Townsend (1Td = 10^{-17} V cm^2)

eV Electron Volt (1eV = 1.6 x 10^{-17} J)

ΔT_{adiab} Adiabatic Temperature Increase (K)

P'' Power Supplied to Reactor (W)

$\dot{V}$ Gas Flow Rate (m s^{-1})

r_{air} Gas Density (kg m^{-3})

$C_{P,air}$ Specific Heat Capacity of Air at Constant Pressure (J kg^{-1} K^{-1})

N Normality of Solution

I_w Current Drawn from Wall (A)

V" Applied Voltage (V)

V' Primary Voltage (V)

I" Secondary Current (A)

I' Primary Current (A)

pf" Secondary Power Factor (dimensionless)

pf Primary Power Factor (dimensionless)

P' Primary Power (watts)

p Pressure (atm)

V Volume (l)

n Number of moles of gas

R Universal gas constant (liter atm $mole^{-1}$ K^{-1})

T Temperature (K)

CHAPTER 1

INTRODUCTION

1.1 Background Information

The Oklahoma Air Logistics Center at Tinker Air Force Base in Midwest City, Oklahoma requires a control technology to reduce the emission of Volatile Organic Compounds (VOCs) from its paint booths, to obtain compliance with Title III of the US Clean Air Act 1990 and MACT (Maximum Achievable Control Technology). Currently, paint with low pigment content is being used to paint aircraft as it has low VOC content. The low pigment paint is not as good in quality as the high pigment paint. Hence, the aircrafts require frequent repainting.

Tinker would like to switch to high pigment paint but the higher VOC emissions results in the need for a control technology. There are of 42 paint booths that operate 5 – 6 hours a day. The entire painting operation is performed in 15 minute intervals. Hence, Tinker needs a control technology that can be turned on and off when required and instantly operate to full capacity.

The general operating characteristics in paint shops have been discussed in detail in the Federal Facilities Sector Notebook [1]. The VOC emission inventory obtained from Tinker is shown in Table 1. The inventory lists the major chemicals emitted from paint booth B2121 and their calculated emission rate in 2001.

TABLE 1.1
Emission Inventory of B2121 Paint Booth Showing
Calculated Values of Annual VOC Emissions

CAS NUMBER	NAME OF COMPOUND	TONNES / Yr
4035-89-6	1,6-Hexamethylene Diisocyanate	0.093
28182-81-2	Aliphatic Isocyanate	0.086
64742-95-6	Aromatic Hydrocarbon	0.071
78-92-2	Sec-Butyl Alcohol	0.057
13463-67-7	Titanium Dioxide	0.055
763-69-9	Ethyl 3-Ethoxypropionate	0.054
123-86-4	Butyl Acetate	0.049
108-10-1	Methyl Isobutyl Ketone	0.045
110-43-0	Methyl N-Amyl Ketone	0.041
108-941	Cyclohexanone	0.025
78-93-3	Methyl Ethyl Ketone	0.015
108-88-3	Toluene	0.012

1.2 Plasma Technology

Conventional VOC control technologies such as thermal incineration, catalytic incineration, and carbon adsorption are costly. At low concentrations, especially, due to strict emission standards, conventional technologies do not offer an efficient and economic solution to VOC abatement. Over the last decade, packed bed plasma and pulsed corona technology has been gaining acceptance as a low cost alternative for treatment of VOCs. As shown by Nunez et al. [2] and Yamamoto et al.[19], it is technically and economically feasible to operate the pulsed corona and packed bed plasma reactors for industrial emission control especially at very low concentrations (less 100 parts per million). Plasma technology also offers other benefits such as ease of operation at ambient temperature, absence of disposal or treatment problems, no possibility of poisoning due to sulfur or halogen containing compounds, and low

maintenance. Also, there is no need to heat the air stream up to temperature of catalyst activity [2].

In previous research conducted at Oklahoma State University studies were performed on destruction of other industrial effluents like methane, tetra chloromethane, hydrogen sulfide, and nitric oxides in AC Dielectric Barrier Discharge (DBD) plasma reactors [8 – 11]. The results prove that AC DBD plasma reactor has the potential for being an effective control technology. The AC DBD reactor can perform as efficiently as the pulsed plasma reactors and also has the added advantage of ease of electrical design. In pulsed plasma systems, high voltage is applied across the reactor in the form of pulses with frequency in nanoseconds. The main drawback of these reactors is high costs of building pulsed voltage generators for industrial uses. Due to these practical problems, pulsed plasma reactors have not been applied in industrial processes [3]. The AC DBD plasma reactor does not require pulsed voltage, which may eliminate expensive electrical circuit design.

1.3 Objectives

The objectives of this study were:

- To obtain the optimum voltage, frequency, and residence time for efficient control of a representative sample of VOCs containing s-butanol, toluene, methyl isobutyl ketone and butyl acetate.
- To obtain the effect of humidity on destruction of VOCs in the AC DBD plasma reactor.

- To obtain downstream ozone concentration for various applied voltages and different values of relative humidity.

1.4 Research Outline

The experimental system consisted of flow controllers, a liquid mixture injection port, a plasma reactor, and influent and effluent sampling ports. Analysis equipment used was an SRI 800C gas chromatograph (GC) with a flame ionization detector.

Initial tests were conducted to select reactor geometry from cylindrical and square plate reactors. Operating parameters were then studied starting with the determination of effect of residence time on destruction while other operating parameters were kept constant. The effect of applied voltage, frequency, and humidity were studied next with flow in the reactor fixed at the optimized residence time and a total VOC concentration of 100 ppm in the reactor. The range of operating parameters is provided in Table 1.2.

TABLE 1.2
Operating Parameters and Their Range

Operating Parameter	**Range**
Primary Voltage	60 – 110 V
Applied Voltage	9463 – 18448 V
Frequency	200 – 400 Hz
Humidity	0% – 80% RH
Residence Time	1.0 s – 0.05 s

Ozone concentration downstream of the reactor was measured at different conditions of voltage, frequency, residence time, and humidity. Results were obtained for variation of ozone concentration with voltage in dry and humid conditions and a comparison was made. Studies were conducted on VOC destruction in different lengths of reactors by increasing the length of outer electrode, and also in multiple tube reactors

with different number of 1 cm and 5 cm long reactors connected in parallel. Power required by reactors of different lengths and different number of reactors in parallel was studied. The effect of reactor length and different number of reactors connected in parallel was also studied on primary and secondary voltage and current.

CHAPTER 2

BACKGROUND AND LITERATURE REVIEW

2.1 Volatile Organic Compounds

Volatile Organic Compounds (VOCs) are comprised of a variety of organic species that are readily reactive in the atmosphere. These compounds have a low boiling point and emit vapors at room temperature. VOCs have been listed as a major source of indoor and outdoor pollution by the EPA due to their presence in numerous household products like cleaning solutions, waxes, disinfectants, stored fuels, paint strippers and other solvents, and their emission from automobiles, paint industries, tanneries, petroleum distilleries, timber, and paper industries [4].

Continuous indoor exposure to VOCs can lead to acute health hazards like damage to liver, kidney, central nervous system and even cancer. Outdoor VOC emission results in production of ground level ozone, which is produced by chemical reaction of VOCs with oxides of nitrogen in the presence of sunlight [5].

Industrial emissions account for 50% of outdoor VOC emission. Due to the damaging health effects of VOCs and the resultant ground level ozone, EPA has strict restriction on their emission. The 8-hour occupational exposure limit for toluene and secondary butanol, for instance, is 100 ppm [6].

2.2 Plasma and Plasma Reactors

2.2.1 Plasma Categorization

Plasma is a collection of free moving electrons and ions that are usually formed upon ionization of gases. To create plasma, energy is required which may be of various forms: thermal, electrical or light energy. Though plasma can be produced and utilized through human technology, it is not a human invention.

2.2.2 Plasma Processing and Plasma Reactors

Electrons in plasma may be in thermodynamic equilibrium with the surrounding gas. Such plasma is defined as equilibrium plasma. Usually such plasma is at a very high temperature, and is often known as *Thermal Plasma*. In industrial processes, the type of plasma used is mainly nonequilibrium plasma where the electrons are not in thermodynamic equilibrium with the surrounding medium. In such cases, the electrons are usually at a much higher energy level than the medium. Normally such plasma is at a lower temperature and usually generated from electrical energy. Such plasma is also known as *Non-thermal Plasma*, or *Non-neutral Plasma* [14].

An important parameter in nonequilibrium plasma is the reduced field, which is defined as the electric field divided by the neutral gas density (E / n). A common unit of measurement of the reduced field is Townsend (Td). One Townsend is 10^{-17} V cm^2. Typically, equilibrium plasmas have very low reduced field (<1Td), as only in such conditions can the electron kinetic energy be comparative to that of heavier particles [14].

Nonequilibrium plasma discharges can be categorized into 5 main classes as explained by Eliasson and Kogelschatz [14] in their plasma technology review. They are explained below.

1. *Glow discharge*: This kind of discharge is formed at low pressures (<10mbar). In this kind of discharge, the electrodes are placed typically in a glass tube. Due to operation at low pressures, it is easy to reach very high reduced fields in this kind of discharge. Hence, the high energy electrons easily excite the neutral atoms and create characteristic glow for each gas. Figure 2.1 shows a typical glow discharge setup.

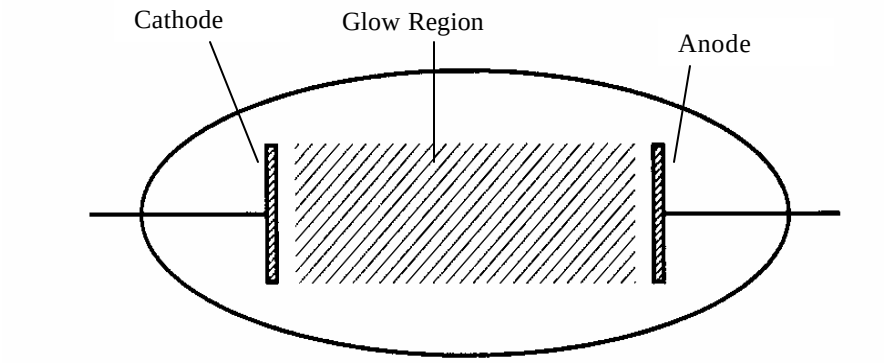

Figure 2.1. Glow Discharge in a Low Pressure Capsule [14].

Glow discharges do not have significant industrial applications in air pollution control due to the low pressures required to sustain them. But they are used extensively in lighting industry in neon and household fluorescent tube lights. Table 2.1 shows the usual operating parameters in glow discharge.

TABLE 2.1

Range of Parameters

in Glow Discharges [14]

Pressure	< 10 mbar
Electric Field	10 V / cm
Reduced Field	50 Td
Mean Electron Energy	0.5 to 2 eV or 5000 – 20000 K
Electron Density	10^{8} to 10^{11} cm^{-3}
Degree of Ionization	10^{-6} to 10^{-5}

2. *Corona Discharge:* To produce stable discharges at normal pressures, inhomogeneous electrode geometries are used. An example of such geometry is the point-to-plate setup shown in Figure 2.2., which produces the corona discharge. It is characterized by a highly localized filamentary glow (corona). Corona can be *positive* or *negative* depending on the whether the charge on the point is positive or negative. The characteristic operating parameters for corona discharges are shown in Figure 2.2. Table 2.2 summarizes the typical parameters required for corona discharge.

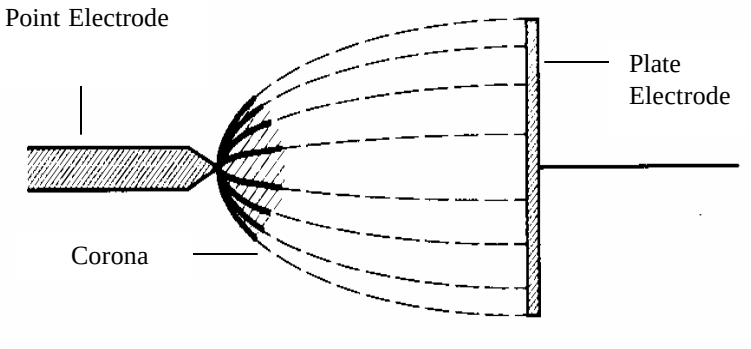

Figure 2.2. Corona Discharge in an Inhomogeneous Geometry [14].

TABLE 2.2
Range of Parameters in
Corona Discharges [14]

Pressure	Atmospheric Pressure
Electric Field	0.5 – 50 kV / cm, variable
Reduced Field	2 – 200 Td, variable
Mean Electron Energy	5 eV, variable
Electron Density	10^{13} cm^{-3}, variable
Degree of Ionization	small, variable

3. *Radiofrequency (RF) Discharge*: Also termed as *Induction Plasma or Electrodeless Plasma,* these kinds of plasma discharges are typical in laboratory analyses in spectroscopic analyses. These discharges are characterized by radio frequencies that range from 2 – 60 MHz. The common industrial frequency is 13.6 MHz. One advantage that these kinds of plasma have over other type of discharges is that the electrodes can be maintained outside the plasma production region. This removes chances of electrode corrosion. Figures 2.3 (a), (b), and (c) show three different arrangements of electrodes to produce RF discharge.

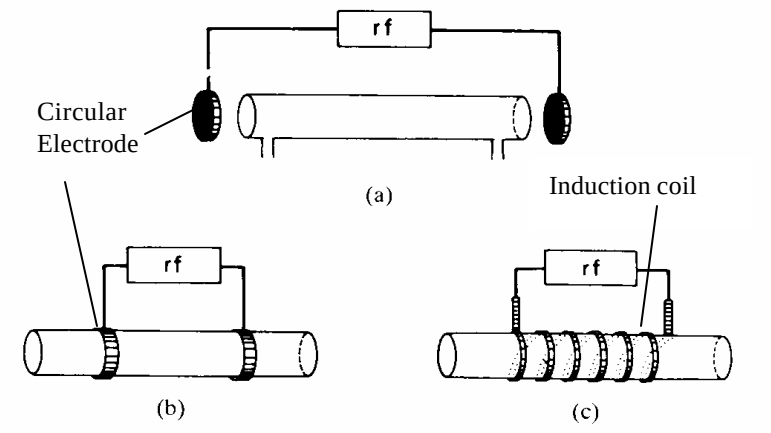

Figure 2.3. Electrode Arrangements in RF Discharges [14].

In Figure 2.3 shown above, arrangements (a) and (b) use capacitive coupling and are mainly used at low pressure. In (a), the electric field is created between the circular electrodes that generates the plasma in the tube. In (b), circular electrodes are wound around the tube, resulting in plasma formation in the tube. Arrangement (c) uses an induction coil, where the solenoid arrangement produces discharge within the reactor.

4. *Microwave Discharge*: These discharges occur in microwave frequencies ranging from 0.3 – 10 GHz. Typical frequencies are 2.45 GHz. Microwave plasmas can be used in a wide range of pressure from 1 mbar to atmospheric pressure.
5. *Silent Electric Discharge or Dielectric Barrier Discharge*: The silent electric discharge is the most commonly used discharge type in industrial processes. This kind of discharge combines the large plasma volume in the glow discharge and the high pressure operation of the corona discharge. In dielectric barrier discharges, a dielectric layer covers at least one of the electrodes. Usually Pyrex, quartz or ceramics are used as the dielectric [16]. The presence of dielectric stabilizes the discharge as the dielectric barrier accumulates the charges on itself once ionization occurs. Hence, the dielectric barrier limits the amount of charge transported by a single micro discharge, and distributes it over the entire electrode, thereby stabilizing the discharge. [17]. Figure 2.4 shows the setup of a dielectric barrier discharge. The topmost and bottom layers are the electrodes. The second layer from bottom is the dielectric barrier, and the second layer from the top is the plasma formation

region. The range of operating parameters of the dielectric barrier discharge is given in Table 2.3.

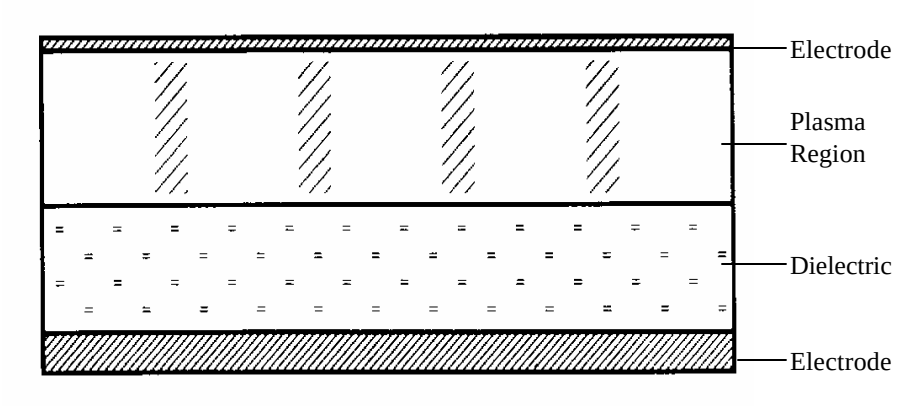

Figure 2.4. Dielectric Barrier Discharge Plasma Reactor [14].

TABLE 2.3
Range of Parameters in
Dielectric Barrier Discharges [14]

Pressure	Atmospheric Pressure
Electric Field	0.1 to 100 kV/cm
Reduced Field	1 to 500 Td
Electron Energy	1 to 10 eV
Electron Density	10^{14} cm^{-3}
Degree of Ionization	10^{-6} to 10^{-5}

Yan et al. [18] classified commonly utilized plasma reactors for industrial research and processes as pulsed streamer corona (PSC), dielectric barrier discharge or silent discharge plasma (SDP), and packed bed corona discharge (PCP). These reactors have been extensively used for VOC decomposition, odor control, flue gas cleaning, CO_2 conversion and biogas and biohazard control. Figures 2.5 and 2.6 show the pulsed corona and the packed bed corona reactor, respectively.

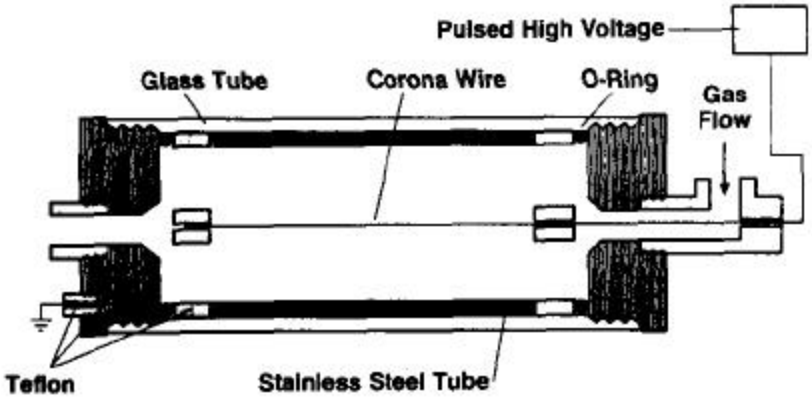

Figure 2.5. Pulsed Streamer Corona Reactor [19].

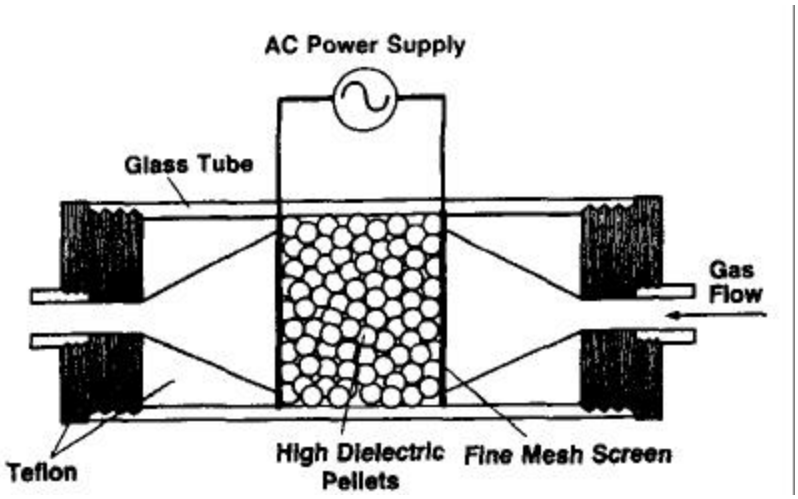

Figure 2.6. Packed Bed Corona Reactor [19].

2.3 Plasma Reactor Characteristics

2.3.1 Plasma Chemistry and Destruction Mechanism

Several theoretical concepts are being developed and evaluated to accurately determine the mechanism of destruction pathways in the plasma

reactor for each compound and also for families of hydrocarbons. The most likely and commonly accepted pathway for VOC destruction is the collision pathway [2]. The electric field in the reactor generates free electrons that undergo both elastic and inelastic collisions as they move through the field. When the electrons have an elastic collision with molecules, they retain most of their kinetic energy. When electrons are accelerated in very strong electric fields, they eventually possess enough energy to have an inelastic collision with molecules. In these collisions the electrons transfer, all or a significant part, of their kinetic energy to the molecules. The following events might occur as the result of such collisions:

- Electrons are attached to electronegative species to form anions.
- Molecular species are dissociated to smaller species resulting in formation of ions or free radicals.
- Molecular and elemental species go into excited states.
- Species are ionized to form positive ions and further free electrons are generated.
- Molecules break down into their elemental components.

The above events depend on the electron energy in the reactor and the type of molecular species present in the reactor. Usually the energy requirement is 5 to 25 electron volts (eV) for the formation of positive ions by electron removal and less than 5 eV for electron attachment and formation of anions [2].

Similar to the above discussed effects, another phenomenon possible in the reactor is photoelectric effect. In photoelectric effects, photon emissions activate the collisions that result in ionization, radical formation, and excitation

that lead to chemical reactions. The electron and proton collisions proceed in similar pathways [2].

The actual development of destruction mechanism requires a lot of information of spatial and time-resolved electron energy distribution function and byproduct formation. There are numerous intermediates that are possible during the destruction of any given VOC in a plasma reactor depending on the nature of the molecular and reactor conditions.

Yan et al. [18] proposed a simplified global mechanism for the destruction of air pollutants in pulsed corona reactors which involves a free radical mechanism. The mechanism is described in the following steps:

1. The first step is *Radical Production*, which is the initiation step in the pathway:

$$M \xrightarrow{K1} R \qquad \text{(i)}$$

2. The following step is the *Pollutant Removal*, which is the propagation mechanism:

$$X + R \xrightarrow{K2} A \qquad \text{(ii)}$$

3. Finally, termination of the reaction takes place in the following possible reactions:

   a) *Radical Linear Termination*

$$R + M \xrightarrow{K3} B \qquad \text{(iii)}$$

   b) *Radical Nonlinear Termination*

$$R + R \xrightarrow{K4} C \qquad \text{(iv)}$$

where R, X, A, B, C and M are radical, pollutant, byproducts and bulk gas compounds respectively. According to them, VOCs follow *Radical Linear Termination*. Using simplifying assumption, they derived the expression for conversion of the pollutant as:

$$\frac{[x]}{[x]_0} = \exp\left(-\frac{E}{b}\right) \qquad (2.1)$$

where [x] and $[x]_0$ are the initial and final concentration of the pollutants, and b is given as:

$$b = \frac{K3 \cdot [M]}{K2 \cdot K1} \qquad (2.2)$$

A possible destruction mechanism for toluene that can be resolved in terms of the above mechanism is given by Nunez et al. [2]. The initial step is the reaction of one of the resonance structures of toluene with excited oxygen species produced in the reactor:

$$C_6H_5CH_3 \longrightarrow C_6H_5CH_2 \xrightarrow{O} C_6H_5\cdot + CH_2O \qquad (a)$$

The benzyl radical in turn reacts with another excited oxygen species to form decomposition products in the propagation reaction:

$$C_6H_5\cdot \xrightarrow{O} O = C\cdot + \cdot C = C - C = C - C = O$$

$$\text{or } O = C = C\cdot + \cdot C = C - C = C \qquad (b)$$

The termination step is the reaction of the O = C· or the O = C = C· radical with another excited oxygen to form CO_2 or CO.

2.3.2 <u>Plasma Physics and Thermodynamic Consideration</u>

One of the most important parameters in determining the extent of total destruction in the plasma reactor is the electric field in the reactor. If the plasma reactor is treated as a capacitor, the electric field in the reactor depends on the geometry [20]. For a square plate reactor, the field is given by:

$$E = \frac{V}{d} \tag{2.3}$$

where V is the applied voltage across the reactor and d is the distance between the electrodes. The electric field is constant in the square plate reactor. But in cylindrical reactors, it depends on the radial distance from the inner electrode as:

$$E = \frac{V}{r \ln\left(\frac{b}{a}\right)} \tag{2.4}$$

where r is the radial distance from the inner electrode, b is the radius of the outer electrode and a is the radius of the inner electrode [20]. The above equations can also be used for dielectric barrier discharge plasma reactors. The energy losses across the dielectrics can be neglected due to the high voltage across the electrodes and low dielectric constant of the material.

Electric field in the plasma reactor determines the initial number of free electrons generated that later propagate further ionic and radical reactions. The electric field may also be used to determine the effect of orientation of polar molecules along the local field lines. This would provide an idea of the total surface area of the molecule that is available for electron impact.

A thermodynamic relationship to compare the total efficiency of different VOC treatment systems is provided by Roland et al. [21]. This can be made on the basis of adiabatic temperature increase which is defined as:

$$\Delta T_{adiab} = \frac{P}{\dot{V} C_{P,air} r_{air}} \qquad (2.5)$$

where P'' is the power supplied to the reactor (W), $\dot{V}$ is the gas flow rate (m s^{-1}), r_{air} is the density of air (kg m^{-3}) and $C_{P,air}$ is the specific heat capacity of air at constant pressure (J Kg^{-1} K^{-1}). According to them, an energetic advantage can be established for the plasma reactor system over other types of VOC abatement systems, but at the present state of the art, this condition is not fulfilled by non-thermal plasma reactors.

2.4 VOC Destruction in Plasma Reactors

2.4.1 VOC Decomposition and Byproduct Formation

Decomposition of VOCs in plasma reactor is accompanied by the formation of numerous organic and inorganic byproducts. Ozone is the common byproduct in plasma reactors operating with air as the feed gas. Yamamoto [22] has listed other common inorganic byproducts in most types of plasma reactors operating with air as the feed gas. They are NO, NO_2, N_2O, CO, and CO_2. Typical trend in VOC decomposition and inorganic byproduct formation is shown in Figure 2.7. According to Yamamoto, two strategies can be used to minimize the formation of inorganic byproducts. One is to minimize the operating voltage of the plasma reactor. Another strategy is to control the oxygen content in air to less than 3% to minimize the emission of NO_x, as this would eliminate the need for secondary control devices.

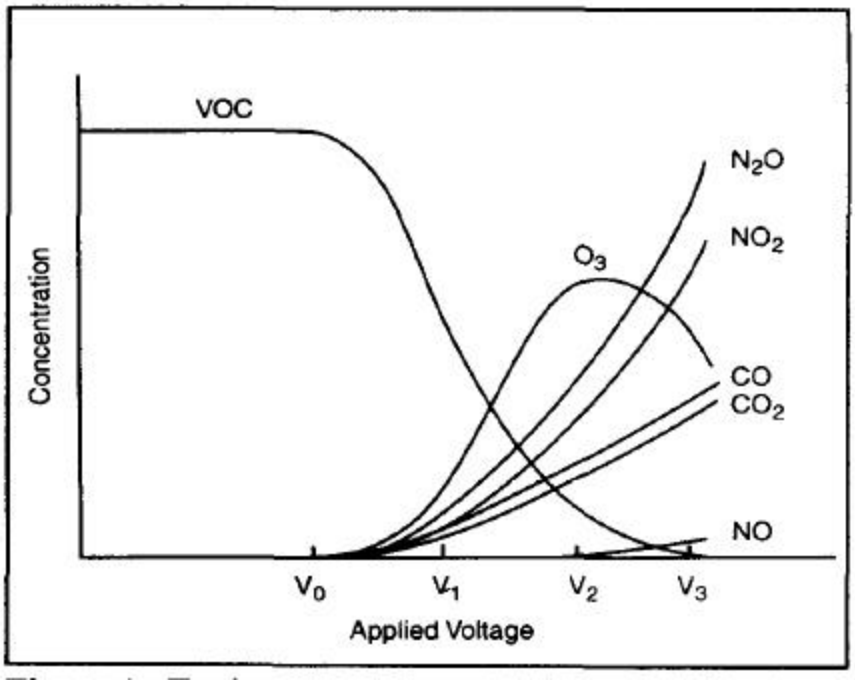

Figure 2.7. Typical VOC Destruction and Formation of Inorganic Byproducts in Plasma Reactors [22].

The formation of both organic and inorganic byproducts is influenced by the type of plasma reactor, plasma operating conditions (applied voltage), and the type of background gases used [22].

2.4.2 Ozone Emission

Ozone is probably the most hazardous of all the byproducts emitted from the reactor. As summarized by Yan [22], the production of ozone as a byproduct observed in previous research initially increase with increase in voltage, then stabilized, and then decreases with further increase in applied voltage (Figure 2.7). Oda [23] also observed a similar trend in emission of ozone (Figure 2.8) while passing pure air and air containing 1000 ppm trichloroethylene (TCE) two

different types of plasma reactors (bolt and coil types). The operating frequency ranged from 50 Hz to 2 kHz ac.

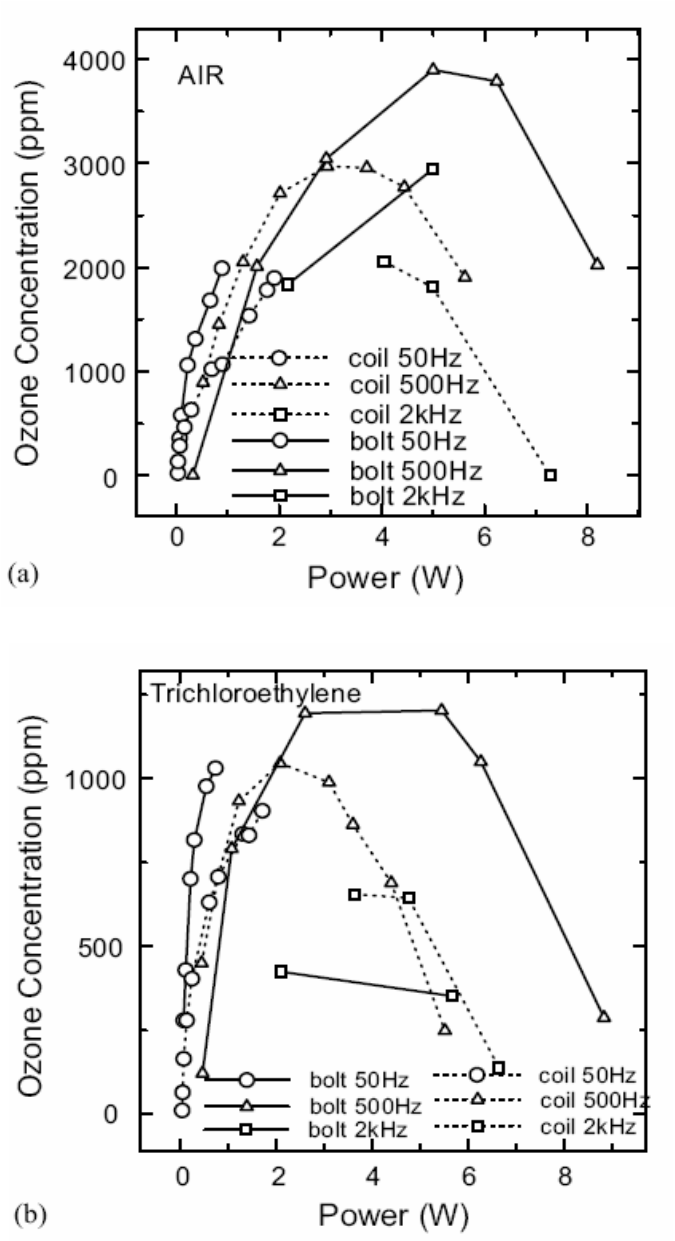

Figure 2.8. Ozone Concentration versus Electrical Discharge Power in Bolt and Coil Type Reactors in (a) Pure Air;(b) 1000 ppm TCE in Air [23]

Numerous other researchers observed similar trends in ozone production while studying the destruction of various VOCs in different kinds of plasma reactors [23].

2.4.3 Effect of Humidity on VOC Oxidation

The presence of humidity has shown mixed effects in different VOC treatment systems depending on the compound that was treated. The presence of humidity was the inhibiting factor in the decomposition of TCE. Hence, the destruction of TCE was optimized in dry air stream. But for case of perchloroethylene (PCE), the presence of humidity enhanced the overall destruction of the compound [24 – 26].

Humidity in a plasma system alters the reaction mechanism as it introduces [OH] species that can also react with molecules to form different intermediates altogether [24 – 27].

2.5 Previous Research at Oklahoma State University in Pollution Control

Previous researchers at Oklahoma State University have used numerous types of single or double dielectric plasma reactors to investigate destruction of common effluents like H_2S, methane, and carbon tetrachloride. Methane destruction efficiency of above 45% was achieved by Piatt [6]. Desai [7] and Magunta [9] achieved H_2S destruction at efficiencies greater than 90%, and Hurst [10] achieved carbon tetrachloride destruction with efficiency above 90%. Parker [11] and Lytle [12] performed studies on

improvement of electrical system used for plasma reactors and recommended electrical design changes for industrial design of plasma reactor.

2.6 Summary

Over the last ten years, plasma reactor technology has been accepted as a better alternative to conventional methods of VOC treatment. Though numerous studies have been conducted on destruction of VOCs in plasma reactors, a comparative study is yet to be performed to develop a common basis to evaluate the different types of plasma reactors used. Such a study would establish the most efficient reactor for a given process, and further research can be concentrated on that reactor.

A generic destruction mechanism with reaction constants that can be used for a wide variety of VOCs is yet to be evolved. The establishment of a single type of plasma reactor as the most efficient of all would provide a direction to a widely digressed study on plasma reactors [18].

CHAPTER 3

EXPERIMENTAL PROCEDURE

3.1 Experimental System

The experimental system was set up as shown in Figure 3.1. Zero grade air was used for studies. A liquid mixture of the VOCs was prepared with secondary butanol, toluene, butyl acetate (all 99+%), and methyl isobutyl ketone (A.C.S reagent grade – 98.5%). The volume ratio in the liquid mixture was calculated to obtain the ratio of the VOCs from the Tinker Emission Database (Table 1.1). The injection rate of the liquid was calculated so that the total theoretical concentration of VOCs in air was near 100 ppm. The liquid was filled in a syringe which was then mounted on the syringe pump. The syringe pump injected the liquid mixture into the air stream at the calculated rate. There was a difference between the theoretical total influent concentration of VOCs and the actual total influent concentration obtained. This is shown in Table 3.1.

TABLE 3.1
Comparison of Expected and Obtained Influent
Concentrations Based on 120 Influent Readings

Compound	**Expected Conc. (ppm)**	**Obtained Average Conc. (ppm)**	**Standard Deviation (ppm)**
S-butanol	43	34.8	3.9
MIBK	26	21.7	2.4
Toluene	8	10.2	3.6
Butyl Acetate	23	16.9	2.8
Total VOC	**100**	**83.6**	**5.6**

Flow rate of air was controlled by a mass flow controller. The reactor was placed in an explosion bay to avoid possible build up of gases and to assure ample room to vent out the downstream exhaust. Power was drawn from a standard 120 V AC, 60Hz wall plug. The power supply, which was connected to the wall, was used to alter primary voltage and frequency as required. The power supply was connected to the transformer which stepped up the voltage to required secondary values for operating the reactor. Primary and secondary voltages, currents and power supplied to the reactor were measured by an electrical data acquisition system. Downstream products were collected into syringes through inline sampling ports and were injected into the gas chromatograph for analysis. Sample injection volume of 0.5 ml was used for analyses. To obtain humidity, the air flow was split into two sections prior to injection of liquid VOC mixture. One section was bubbled through to make it a saturated humid stream and the other was dry. Both the flows were then combined and continued to the liquid injection port. The ratio of flow rates of the split flows were varied, keeping the total flow rate constant, until the correct humidity was achieved.

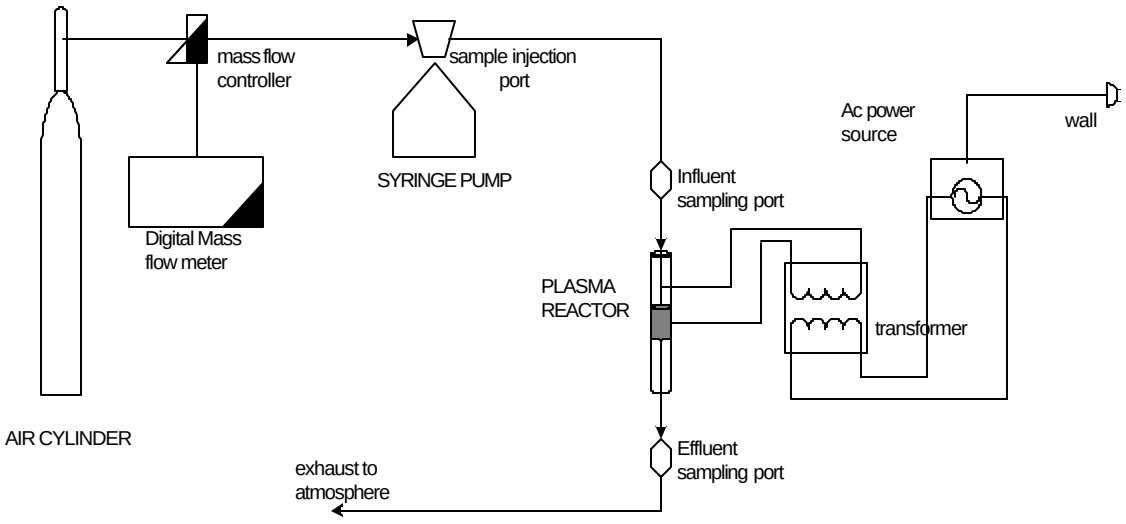

Figure 3.1. Experimental Setup

3.2 Equipment Specification

3.2.1 Dielectric Barrier Discharge (DBD) Plasma Reactor

The shape of the reactor is an important factor in determining the electric field inside the reactor. Previous studies at Oklahoma State University were performed with a cylindrical shaped reactor with an annular space between two concentric electrodes. In this test, a cylindrical reactor and a flat plate reactor were considered, as the electric field distribution in the two reactors is different.

The property of the dielectric material is another important factor that affects the voltage and electric field inside the reactor. Quartz glass and Teflon were selected as dielectric materials. Three reactors were constructed with different configurations. A double dielectric barrier cylindrical reactor with both inner and outer electrodes in contact with quartz, a single dielectric barrier reactor with only the outer electrode in contact with quartz, and a flat plate reactor with both electrodes covered by Teflon.

The cylindrical reactor was constructed with copper tape as the outer electrode, wound around quartz tube that acts as the outer dielectric. The tape was wound to the required length of the outer electrode. A thin copper rod acts as the inner electrode. In the double dielectric reactor, the copper rod was fitted in a quartz tube that had the same inner diameter as the outer diameter of the rod. The rod was placed at the annulus of the quartz tube.

Flat plate reactor was constructed with two copper plates placed between flat Teflon layers so that there was a gap for flow of gases. The shell of the reactor was made with Pyrex glass. The single dielectric plasma reactor is shown

in Figures 3.2. The ends of the tube are fixed to Pyrex plates with gaskets to obtain airtight connection. The outer electrode is connected to the high voltage end of the transformer. Plasma formation inside the reactor can be seen in Figure 3.3. The flat plate reactor is shown in Figure 3.4. Tables 3.2 and 3.3 list the specifications of the cylindrical and flat plate reactors.

A multiple tube reactor was constructed by connecting the required number of reactors in parallel, with a maximum capacity of ten tubes. The tubes were enclosed in a shell, and the ends of the tubes passed through discs with circular spaces equal to the outer diameter of the quartz tube. The discs were fixed to the ends of the reactor shell, and gasket – sealed to obtain airtight connection. The reactors in the multiple tube reactor were electrically connected in parallel. The electrical connection was achieved by winding copper wire around all the electrodes and leaving the end of the wire to connect to the transformer. Figures 3.5 and 3.6 show the multiple tube reactor.

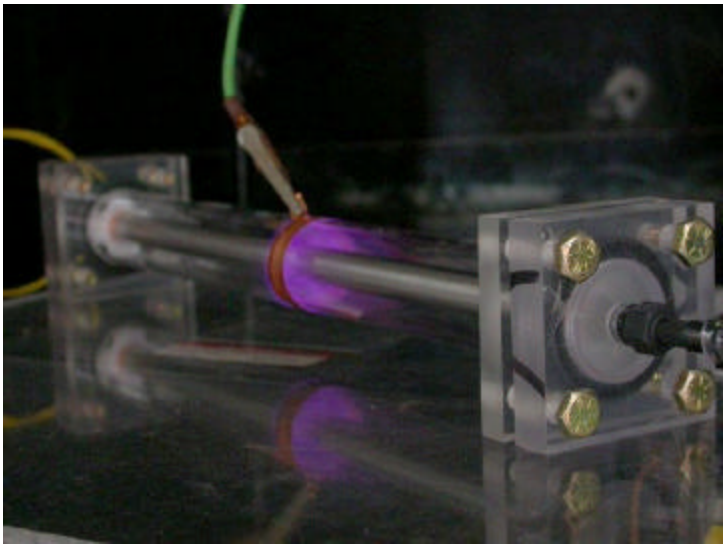

Figure 3.2. Single Dielectric Barrier Discharge Plasma Reactor [28]

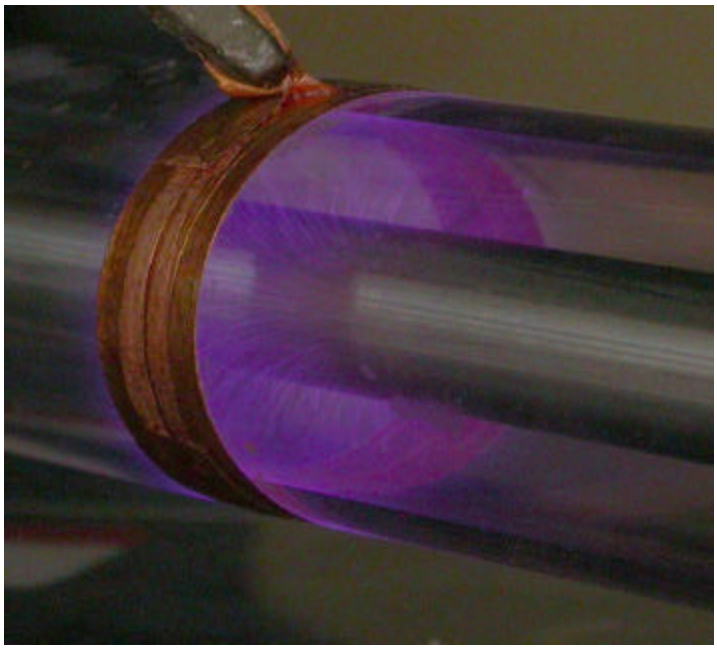

Figure 3.3. Plasma Formation in Dielectric Barrier Discharge Plasma Reactor [28]

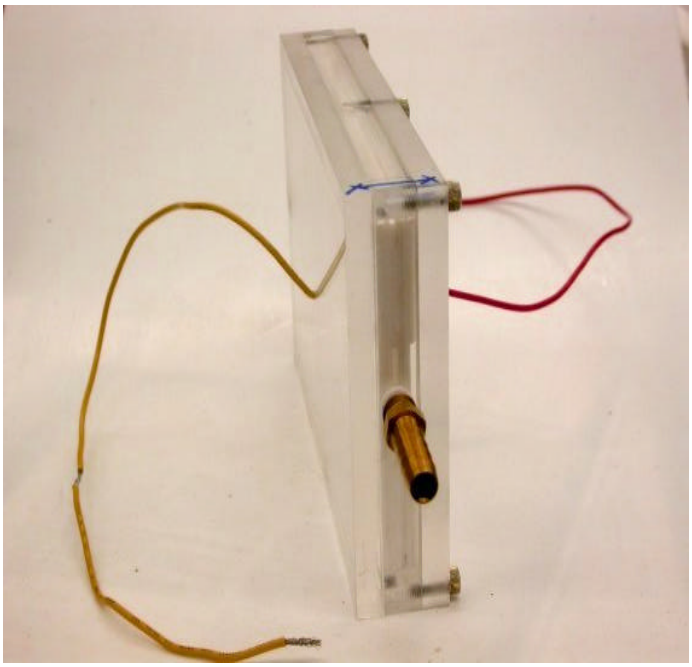

Figure 3.4. Flate Plate Reactor [28]

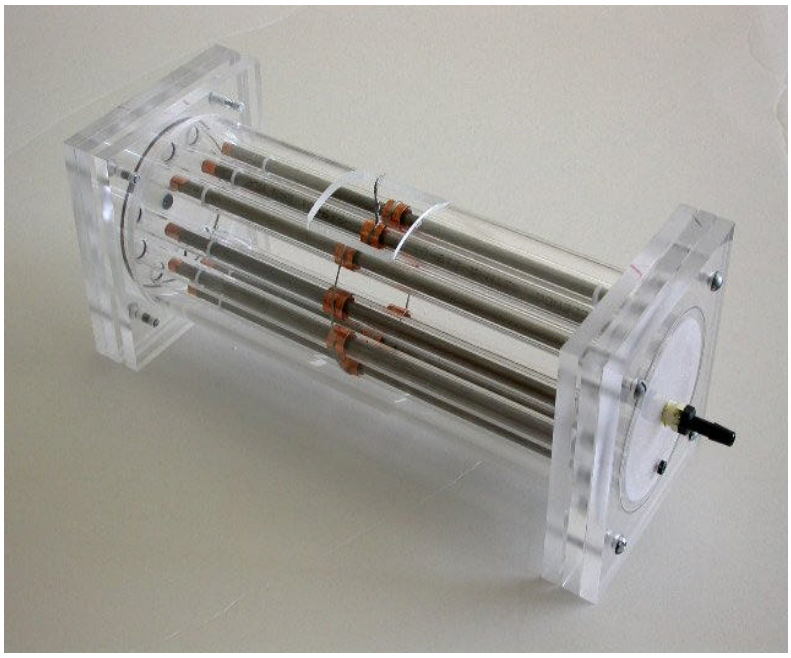

Figure 3.5. Multiple Tube Single Dielectric Plasma Reactor [28]

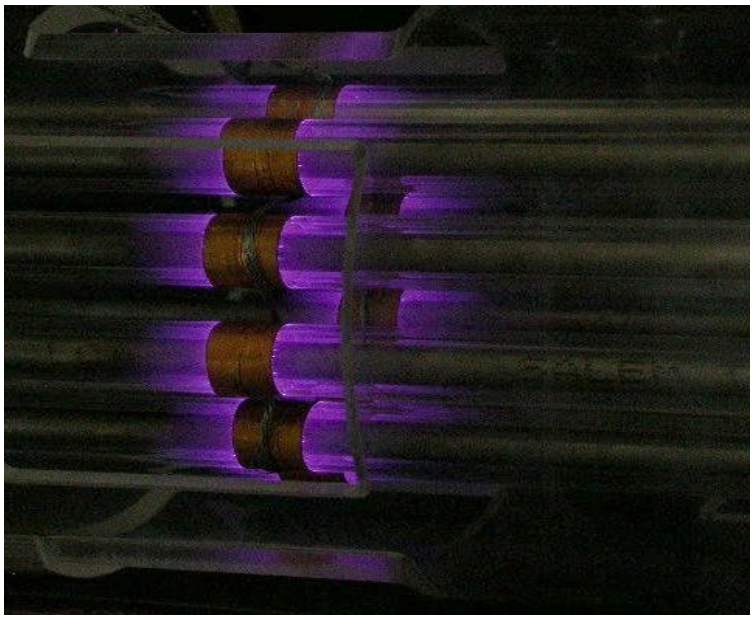

Figure 3.6. Plasma Formation in Multiple Tube Reactor [28]

TABLE 3.2
Cylindrical Reactor Dimensions

Specification	Single Dielectric	Double Dielectric
Inner electrode diameter	¼ inch	¼ inch
Inner dielectric ID	NA	¼ inch
Inner dielectric OD	NA	7 mm
Outer dielectric ID	10mm	10 mm
Outer dielectric OD	11.59 mm	11.59 mm
Tube length	11 inches	11 inches

TABLE 3.3
Flat Plate Reactor Dimensions

Length	5.375 cm
Width	3 cm
Dielectric thickness	0.17 cm
Gap	0.17 cm

3.2.2 Mass Flow Controllers

Two Brooks TR Series mass flow controllers, labeled M1 and M2, and a rotameter were used to control the flow rate of air. The mass flow controllers were connected to a Linde FM 4575 mass flowmeter. Calibration of M1, M2 and the rotameter are shown in Appendix A. M1 and M2 were connected to the mass flowmeter as required. The numerical value set on the panel of the mass flowmeter corresponded to the calibrated flow rate through the mass flow controllers. The flow rate through the rotameter was adjusted by changing the height of the ball. M1 and M2 were calibrated against an Altech Digital Flow Meter and the rotameter was calibrated with a wet flow meter. Figure 3.7 shows a mass flow contoller and Figure 3.8 shows the Mass Flowmeter. Calibration plots of the mass flow meters are provided in Appendix A.

Figure 3.7. Brooks 5850TR Mass Flow Controller

Figure 3.8. Linde FM 4575 Mass Flowmeter

3.2.3 Gas Chromatograph

An SRI 8610C gas chromatograph (GC) with Flame Ionization Detector (FID) was used for analyses. Helium was the carrier gas at a flow rate of 20 sccm. Air at 200 sccm and hydrogen at 20 sccm were used as combustion gases. The GC was fitted with a 25 ft Restek™ customized capillary column for analysis of VOCs, and connected to a computer with installed software to read the output of analyses. Samples were injected into the GC using a Hamilton 1002SL 2.5 ml sample lock syringe into the on-column injector.

The GC was calibrated for the VOCs using a standard mixture of 100 ppm of each component in air. The standard mixture was purchased from Scott Specialty Gases™. Starting from 0.01 ml of the sample, injections were made in increments of 0.01 ml, up to 0.1 ml. Then, the mixture was injected with 0.1 ml increments up to 0.8 ml. Integrated areas in the GC corresponded to calibrated values of mass fractions. Figure 3.9 shows the GC. Operating specifications for the GC are provided in Table 3.4. The calibration curve of the VOCs is provided in Appendix C.

TABLE 3.4
GC Operating Specifications

Column temperature	70 ^{o} C
Injector temperature	70^{o} C
FID temperature	375 ^{o} C
Carrier gas	Helium (20 sccm)
Combustion gas	Hydrogen (20 sccm)
Combustion gas	Air (200 sccm)

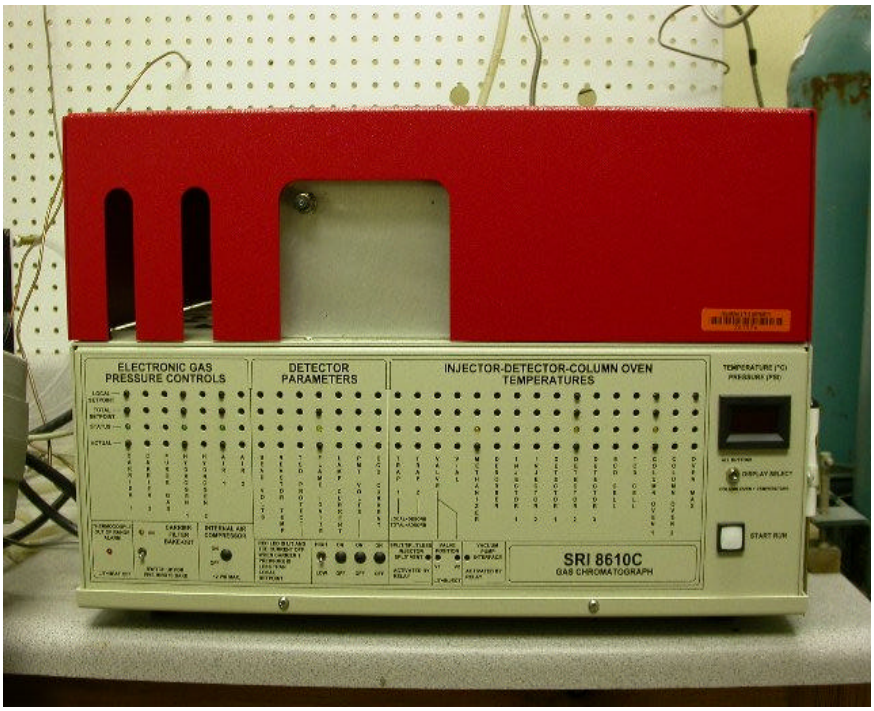

Figure 3.9. SRI 8610C Gas Chromatograph

3.2.4 Temperature Measurement

Two Omega type K thermocouples were used for temperature measurement. One thermocouple was fixed inline following the liquid injection port to observe temperature inside the room and the other was fixed at the reactor exit the measure temperature of downstream products. The thermocouples were connected to an Omega DP465 temperature probe, which is shown in Figure 3.10.

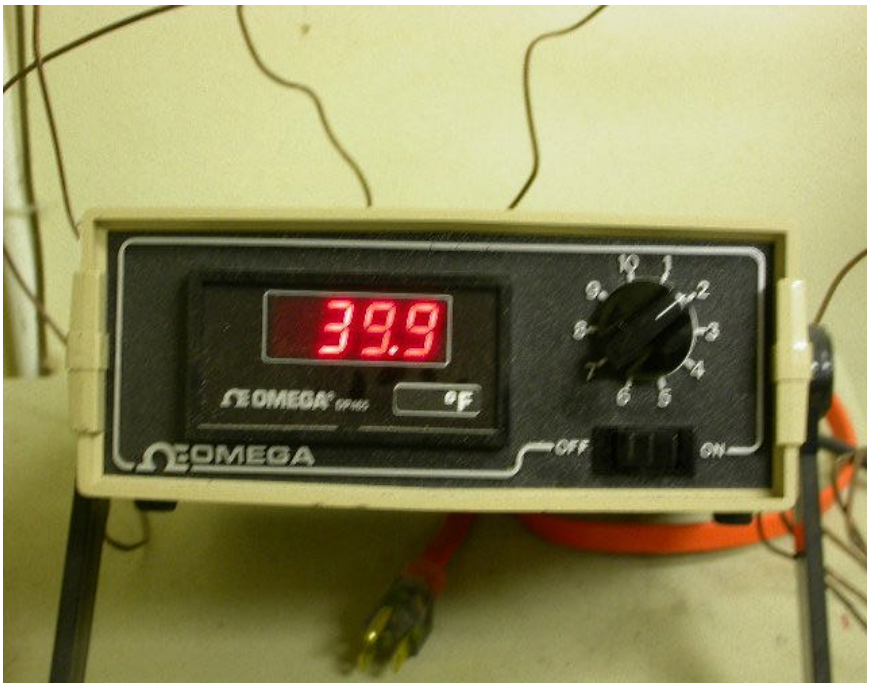

Figure 3.10. Omega Temperature Probe

3.2.5 Power Supply

California Instruments Model 1001TC AC Power Source (Figure 3.11) was used to regulate voltage and frequency on the primary side. The power supply was connected to a standard 120 V AC, 60 Hz wall plug.

3.2.6 Transformer

The primary voltage was stepped up to secondary high voltage using a Franceformer Model 15060P center tap transformer shown in Figure 3.12. The transformer is designed to provide an output of 15 kV, 3VA for a 120 V AC and 60 Hz wall input.

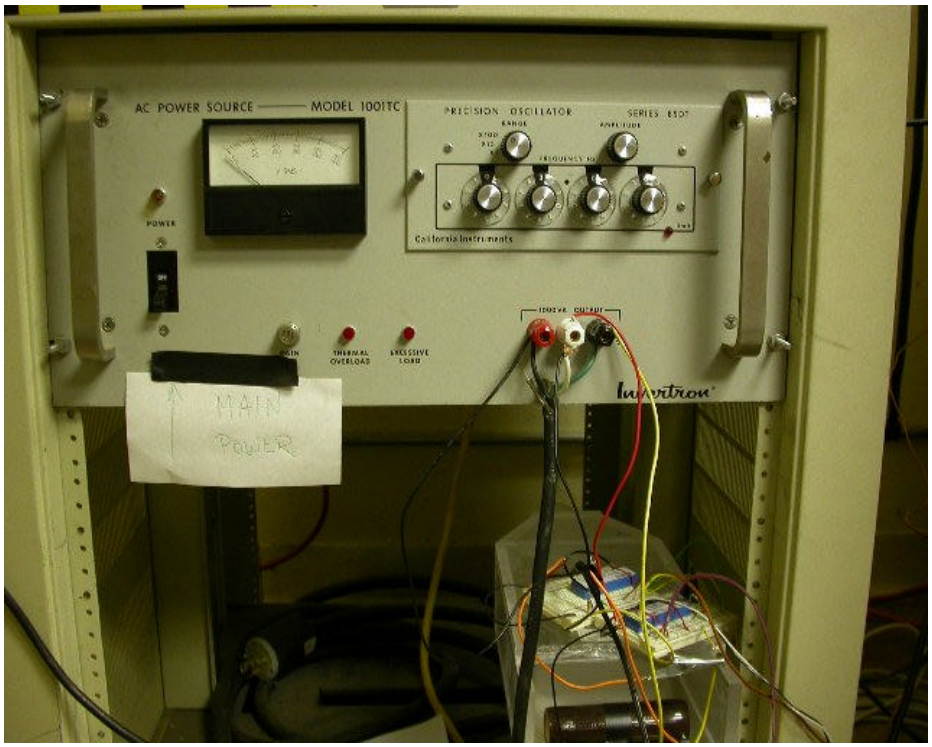

Figure 3.11. California Instruments 1001TC AC Power Source

Figure 3.12. Franceformer Model 15060P Transformer.

3.2.7 Electrical Measurements

Secondary current was measure using an optical isolator. Two LEDs were used as both the electrodes of the reactor were energized. One LED was forward biased and the other was reverse biased to detect current in both directions. Each LED was isolated from a separate phototransistor using a 1 mm thick borosilicate glass plate. The ends of both the phototransistors were connected to a single resistor. The reactor current was then calculated by measuring the voltage across this resistor. This was a slight modification from the method used by Feng et al. [29] Secondary voltage was measured using a voltage divider circuit similar to that explained by Feng et al. Power factor to the reactor was calculated by measuring the phase angle between the secondary voltage and current. All the electrical data were read through a National Instruments™ data acquisition board using the Lab View (version 7.0) software.

Secondary current and secondary voltage measurement circuits used in this study are shown in Figures 3.13 and 3.14, respectively. The data acquisition board and the dc power supply for electrical measurement circuit are shown in Figures 3.15 and 3.16. All the electrical circuits used in this study were developed by Ms. Visalakshi Annamalai, an Electrical Engineering Graduate student at Oklahoma State University.

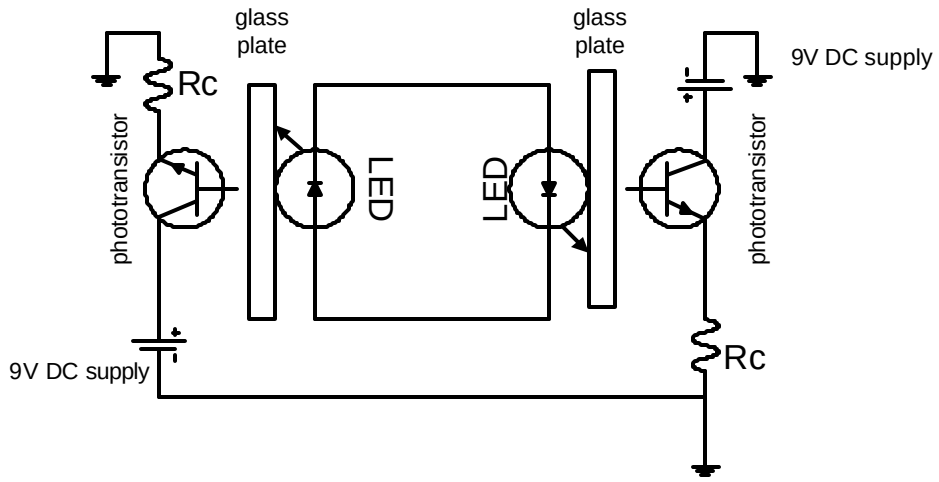

Figure 3.13. Optical Isolator Circuit to Measure Secondary Current

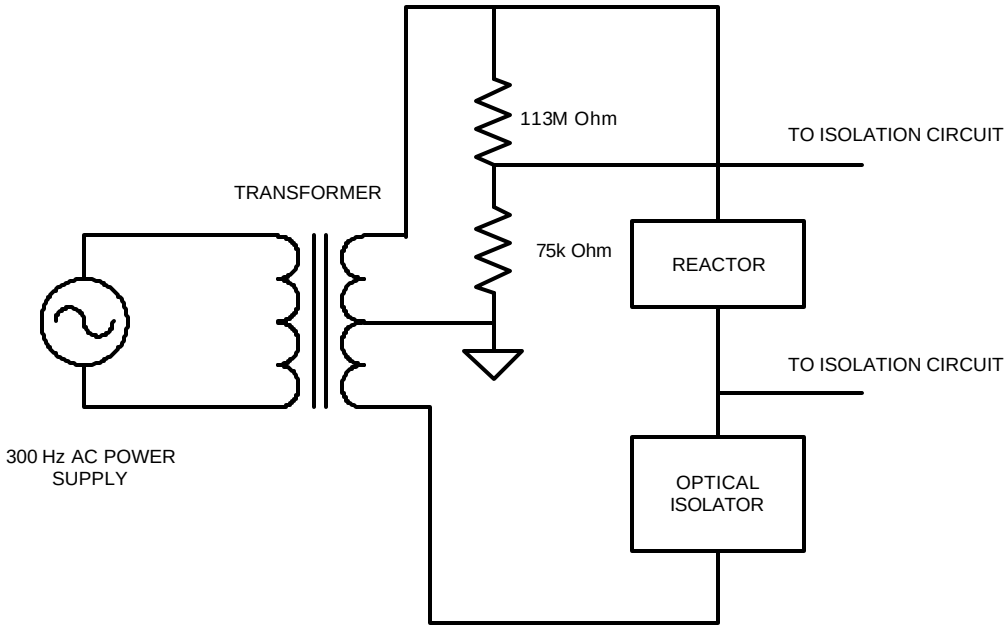

Figure 3.14. Voltage Divider Circuit for Secondary Voltage Measurement

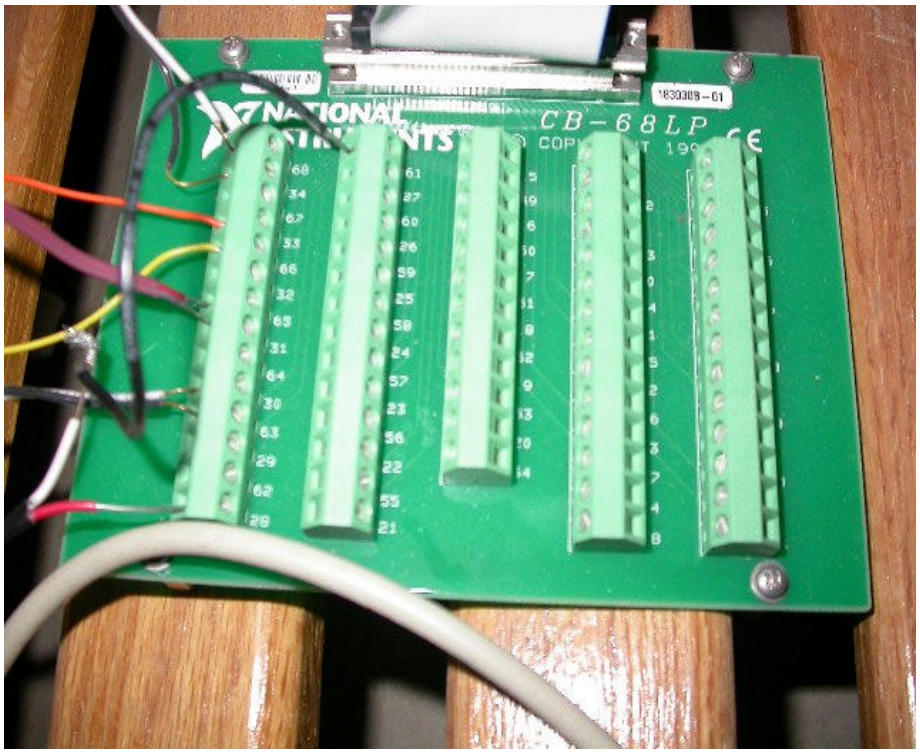

Figure 3.15. National Instruments Electrical Data Acquisition Board

Figure 3.16. BK Precision 1710 DC Power Supply.

3.2.8 Syringe Pump

A Harvard Apparatus Model '22' syringe pump was used to inject the liquid mixture of VOCs into the air stream at the liquid injection port. The injection rate of the syringe pump ranged from 0.02 µl/min to 10 ml/min. Figure 3.17 shows the syringe pump.

Figure 3.17. Harvard Apparatus Model '22' Syringe Pump.

3.3 Experimental Procedure

Prior to commencement of the experimental procedure, certain safety precautions are to be followed. They are listed below.

1. As the transformer operates at high voltages, an inspection should be made to insure there are no open lead wires and no metallic objects in the vicinity of transformer outputs.

2. The MSDS of all materials should be checked and made up to date. The MSDS are kept in the laboratory folder next to the door.
3. Connections should be checked and insured against leaks. Downstream exhaust gases must be safely vented out into the atmosphere by using a long exhaust pipe the extends outside the explosion bay.
4. As the outer electrode of the reactor is also energized, there might be ozone production due to interaction of the outer electrode with atmospheric oxygen. Care should be taken not to spend too much time in the reactor vicinity to prevent exposure to ozone.

With all the safety precautions observed and the experimental setup ready, the detailed experimental procedure is given below.

1. Set the mass flow controller to obtain the desired flow rate of air.
2. Open the helium, air and hydrogen cylinder valves to allow their flow through the GC, and turn on the GC and the FID. Set the GC and FID temperatures to the values listed in Table 3.4, and allow time for the GC to attain the operating conditions.
3. Inject the liquid mixture of secondary butanol, methyl isobutyl ketone, toluene, and butyl acetate into the air stream at the sample injection port using the syringe pump. The injection rate is set at a previously calculated value to achieve a total required concentration of VOCs in the air stream. Injection port should be maintained at a higher temperature (65^{o} C) to vaporize all volatile components.
4. Collect influent samples and inject in the GC until consistent values are obtained in the chromatogram, to confirm that the feed is at constant composition.

5. Commence destruction by turning on the power source to energize the reactor and set the primary voltage and frequency at the required value.
6. Collect 0.5 ml effluent gas samples once the reactor is on through the sampling port downstream of reactor. Inject the sample into the GC.
7. The GC output chromatogram is recorded in the computer. Convert the areas of individual peaks in the chromatogram to mass fractions of individual compounds from calibration data.
8. Repeat steps 3 through 7 to perform another experiment after purging the reactor and setting the necessary condition for the experiment.
9. To shutdown the process, turn off the power supply after decreasing the amplitude of the primary voltage. Turn off the syringe pump and the air feed to the reactor. Turn off the GC gases and then switch off the GC.

3.4 Ozone Measurement

Standard iodometric titration method was used to estimate the downstream ozone. The method is described in APHA, AWWA, and WPCF book for standard methods [30]. The titration procedure is given below

3.4.1 Apparatus for Ozone Collection

1. A standard gas – washing bottle of 500 ml capacity for ozone collection.
2. Standard titration apparatus consisting of 50 ml burette on burette stand 500 ml titration flask.

3.4.2 Reagents

1. Potassium iodide (KI) solution: Dissolve 20g of KI in 1 l freshly boiled and cooled distilled water, and store in brown bottle.
2. Sulfuric acid (H_2SO_4), 1 *N*.
3. Standard sodium thiosulfate ($Na_2S_2O_3$), 0.005 *N*: Dissolve 25 g of $Na_2S_2O_3$? 5 H_2O in 1 l freshly boiled and cooled distilled water. Dilute 50 ml of this solution to 1000 ml.
4. Starch indicator solution: Add distilled cold water to 5g potato to form a thin paste. Pour this paste into 1 l boiling distilled water, stir, and allow to settle overnight. Use the clear supernatant. Preserve with 1.25 g salicylic acid.

3.4.3 Procedure

Pour 400 ml of the KI solution in the gas – washing bottle. Collect the downstream gas into this bottle for about 45 s to 1 min. The solution turns yellow due to liberated iodine. Transfer the KI solution into the titration flask and add 20 ml of sulfuric acid. Titrate the solution against the thiosulfate until the yellow color of the liberated iodine almost disappears. Add 4 ml of starch indicator. The solution will now turn blue. Continue titration rapidly but carefully till the blue color is just discharged. The concentration of ozone in the collected sample is calculated according to Equation 3.1.

$$O_3\left(\frac{mg}{l}\right)=\frac{V\times N\times 24000}{Vsample} \qquad (3.1)$$

Where V is the volume of thiosulfate required for titration, *N* is the normality of the thiosulfate solution (0.005), and *Vsample* is the volume (in ml) of the downstream sample collected (calculated by multiplying the flow rate of the downstream gas and the time of collection). The ozone concentration, in ppm, can be obtained from the ideal gas law in the following way:

$$pV = nRT \tag{3.2}$$

where p is pressure (1 atm), *V* is the volume (1 liter), R is the universal gas constant and T is temperature (assumed to be constant at 25 ^{0} C during the runs). The value of *n* is obtained as 0.041 moles. Hence, the concentration of ozone, in ppm, can be calculated as follows:

$$O_3 \text{ (ppm)} = O_3\left(\frac{mg}{l}\right) \text{x} \left(\frac{1}{48}\right) \text{x} \left(\frac{1}{0.041}\right) \text{x } 1000 \tag{3.3}$$

Experiments were performed by varying the values of voltage, frequency, humidity, and residence time. The effect of each parameter on destruction was studied, and ozone concentration was observed under different conditions. The results of the experiments have been discussed in Chapter 4.

CHAPTER 4

RESULTS AND DISCUSSION

4.1 Selection of Geometry and Dielectric Material

The cylindrical dielectric barrier reactor was selected for study due to ease of construction and operation. Quartz glass was selected as the dielectric material due to its high dielectric strength and low dielectric constant. Teflon was rejected due to its low operating temperature range and also because Teflon vapors are harmful if inhaled. The properties of Teflon and quartz glass are listed in Table 4.1.

TABLE 4.1
Properties of Teflon and Quartz

Material	Dielectric Constant	Dielectric Strength (V / m)	Max. Continuous Operating Temp. (^{o}C)
Teflon	4.1	1.8×10^{7}	260
Quartz	3.75	5×10^{7}	1120

During preliminary tests, the overall destruction of VOCs in the single dielectric barrier reactor was higher. Hence, the single dielectric barrier reactor was selected for further tests. Figures 4.1 and 4.2 show the destruction of VOCs in the single and double dielectric reactors. The overall VOC destruction (at sampling time of 23 min after the reactor was turned on) was 89 % in the double dielectric reactor, and 95 % in the single dielectric reactor. The overall VOC destruction is the percentage of the total number of

VOC molecules that are oxidized in the reactor. The effluent concentration reached a steady value around 23 minutes after the reactor was energized. Hence, in latter studies, the effluent concentrations obtained for samples drawn at 23 minutes were regarded as the equilibrium outlet concentrations.

The initial effluent sample was drawn 30 seconds after the reactor was switched on, as the time required for the first batch of oxidized gas to reach the effluent port was calculated as 30 seconds for a residence time of 1 second. Also, it takes at least 20 seconds or more for a person to reach the effluent port in the explosion bay after switching the reactor on from inside the laboratory.

Figures 4.1 and 4.2 are destruction plots that show the fraction of initial concentration remaining of individual VOCs and overall influent at 30 s, 2 minutes, 8 minutes, 15 minutes, and 23 minutes after the reactor was switched on. The reactor was switched off at 23 minutes. The values at 30 minutes and 35 minutes show the VOC concentrations returning to the influent values after the reactor was turned off.

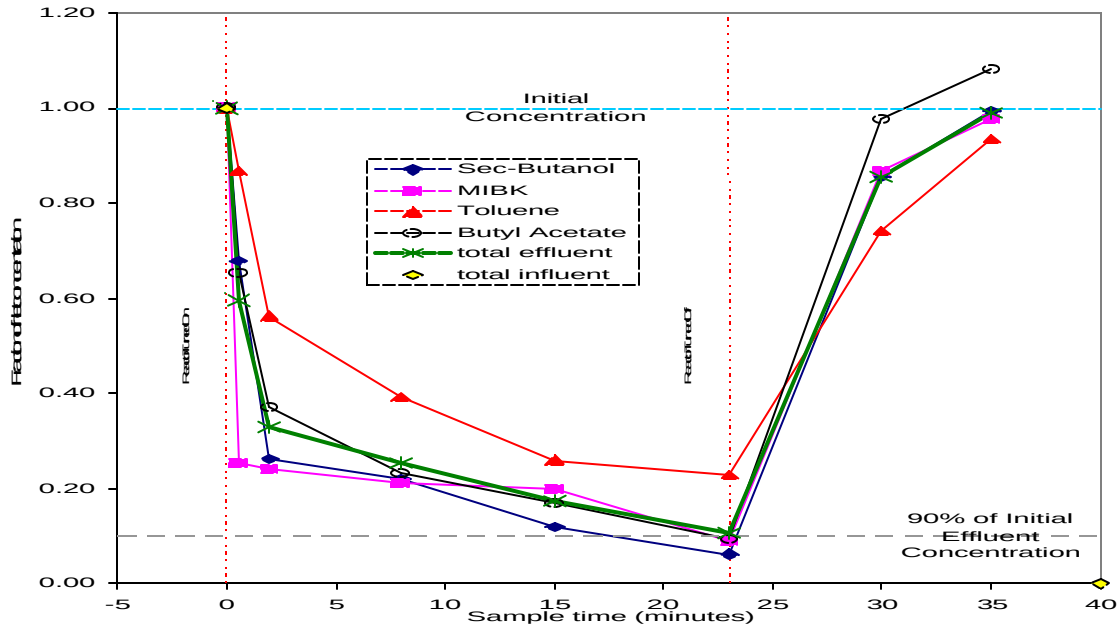

Figure 4.1 Destruction of VOCs in double dielectric barrier reactor at 15 kV, 300 Hz, and τ = 1 s.

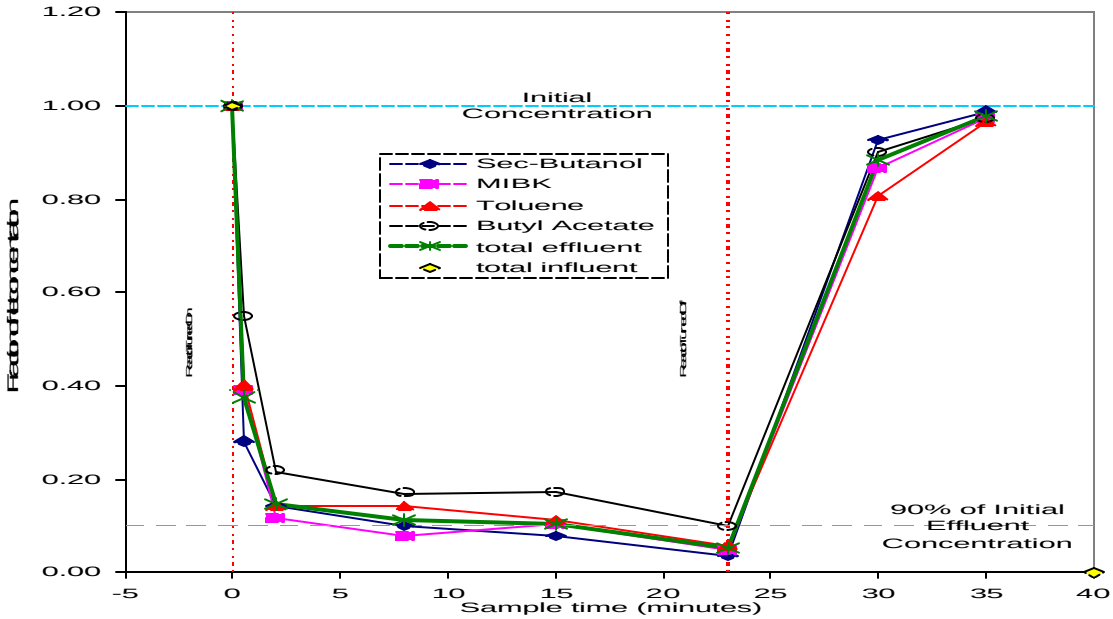

Figure 4.2 Destruction of VOCs in Single Dielectric Barrier Reactor at 15 kV, 300 Hz, and τ = 1 s.

The effects of residence time, voltage, frequency and humidity on the destruction of VOCs and the concentration of ozone downstream of the reactor have been addressed in the following sections.

4.2 Residence Time

Initial tests were conducted with decreasing residence time by increasing the flow rate of influent VOC mixture through the 1 cm long single dielectric barrier reactor. Overall VOC destruction increased as the residence time decreased to 0.2 s, beyond which the overall destruction started to decrease. Hence, 0.2 s was selected as the optimum residence time. The overall destruction of VOCs with respect to residence time is given in Table 4.2. All the destruction results shown in this chapter are average values of three runs conducted under same conditions. The results were repeatable within ± 10%

in all the destruction runs. Figure 4.3 shows the variation in overall destruction of the VOCs with respect to the residence time.

TABLE 4.2
Overall VOC Destruction vs. Residence Time at 15 kV and 300 Hz

Flow rate (ml / min)	Re	Residence Time (t) in s	% VOC Destruction				
			S-butanol	MIBK	Toluene	Butyl Acetate	Overall
47	4	0.6	68 %	86 %	84 %	78 %	77 %
70.5	5.9	0.4	83 %	87 %	93 %	95 %	89 %
141	11.7	0.2	92 %	97 %	89 %	97 %	94 %
282	23.4	0.1	60 %	97 %	90 %	93 %	80 %
564	46.8	0.05	56 %	89 %	85 %	83 %	74 %

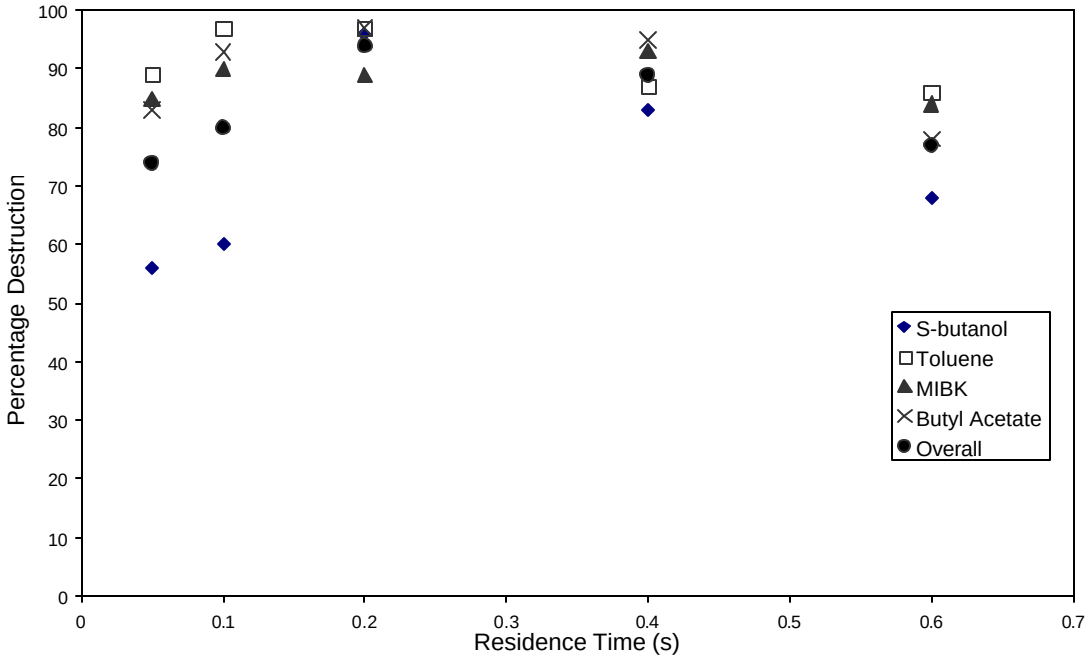

Figure 4.3. Destruction of VOCs versus Residence time Single Dielectric Barrier Reactor at 15 kV, 300 Hz.

The destruction trend, seen in Figure 4.3, was different from what was expected. The expected trend was that decreasing the residence time would decrease the overall destruction of VOCs, especially at flow rates with low Reynolds numbers, where mixing effects would not affect the oxidation of the VOCs greatly. The destruction plots for different residence times are shown in Figures 4.4 through 4.8. Though the reactor was initially expected to display "instant on and off" properties, the destruction plots seem to suggest otherwise. The effluent concentration gradually attained a steady value, instead of immediately reaching a steady outlet concentration.

In similar tests conducted previously, different researchers obtained different results. In studies conducted by Yan et al. [18], residence time had no significant effects on VOC destruction. But according to Yamamoto [22], the destruction of VOCs increased with increase in residence time.

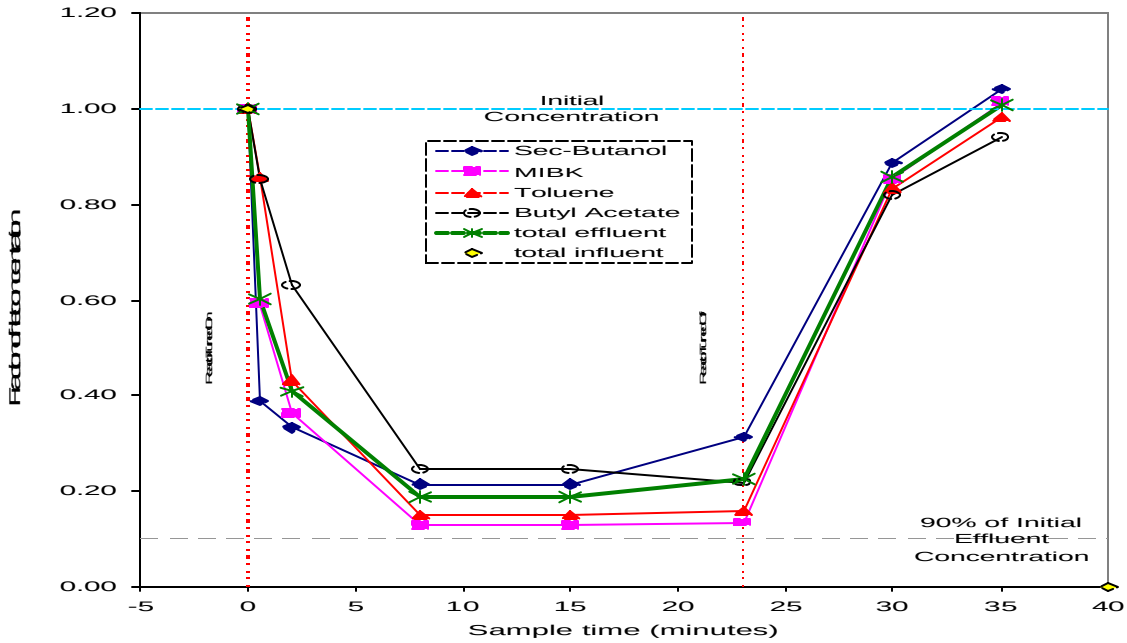

Figure 4.4 Destruction of VOCs in Single Dielectric Barrier Reactor at 15 kV, 300 Hz, and τ = 0.6 s.

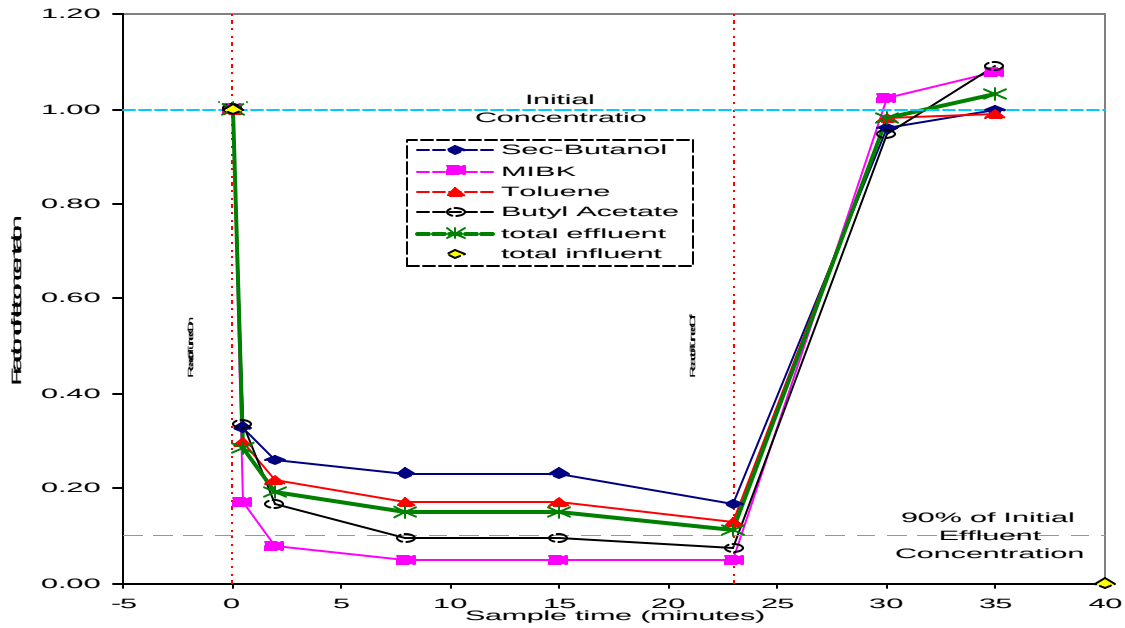

Figure 4.5 Destruction of VOCs in Single Dielectric Barrier Reactor at 15 kV, 300 Hz, and τ = 0.4 s.

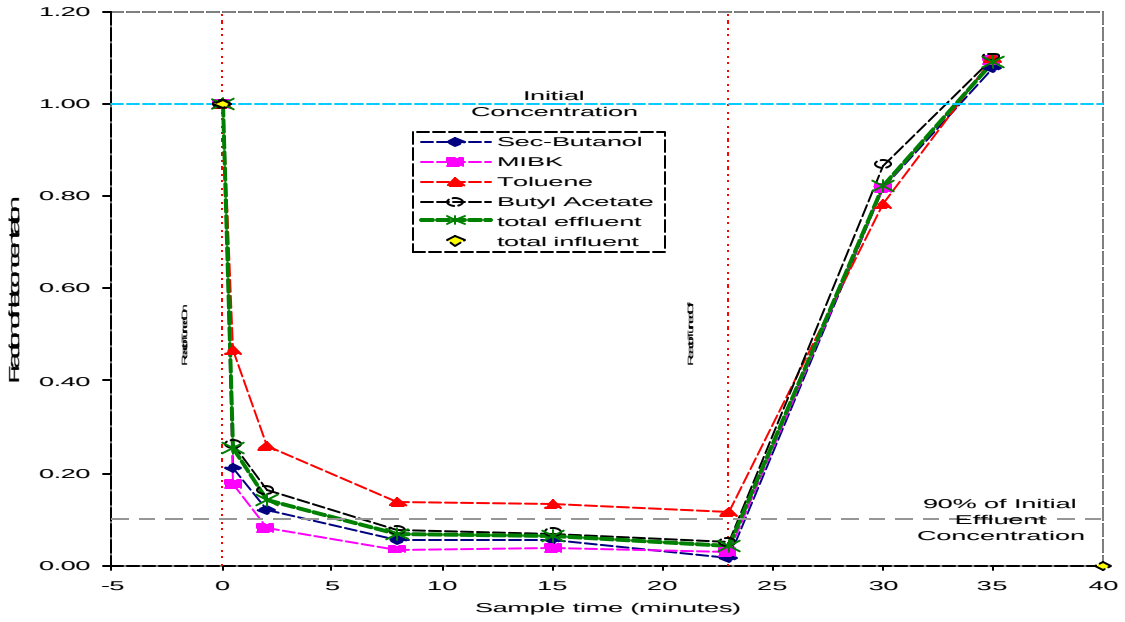

Figure 4.6 Destruction of VOCs in Single Dielectric Barrier Reactor at 15 kV, 300 Hz, and τ = 0.2 s

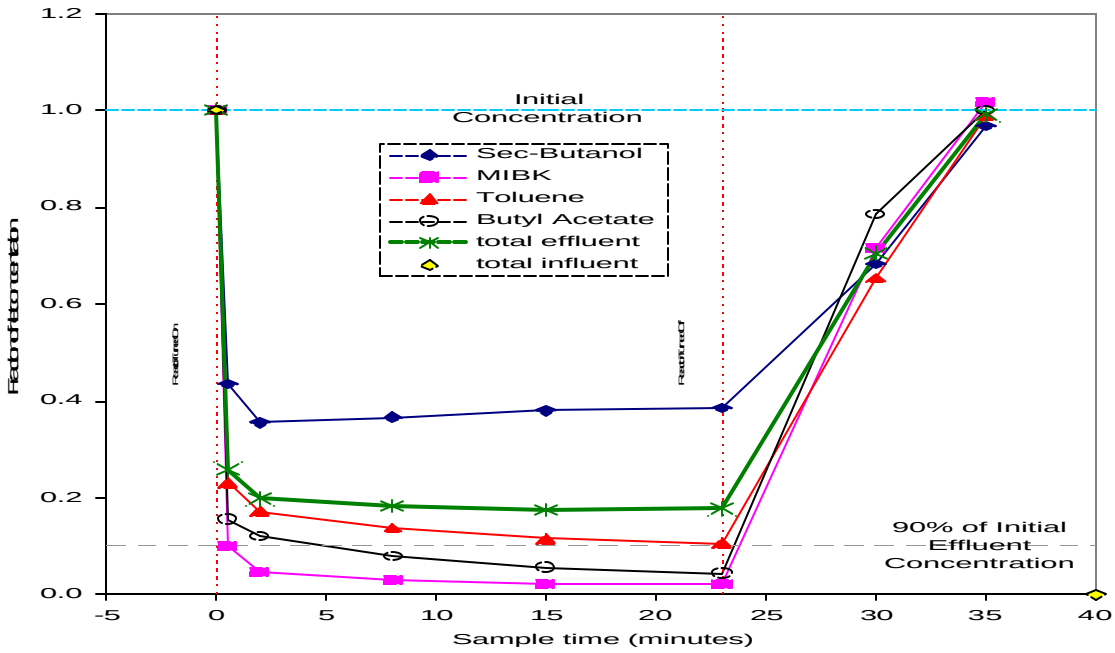

Figure 4.7 Destruction of VOCs in Single Dielectric Barrier Reactor at 15 kV, 300 Hz, and τ = 0.1 s

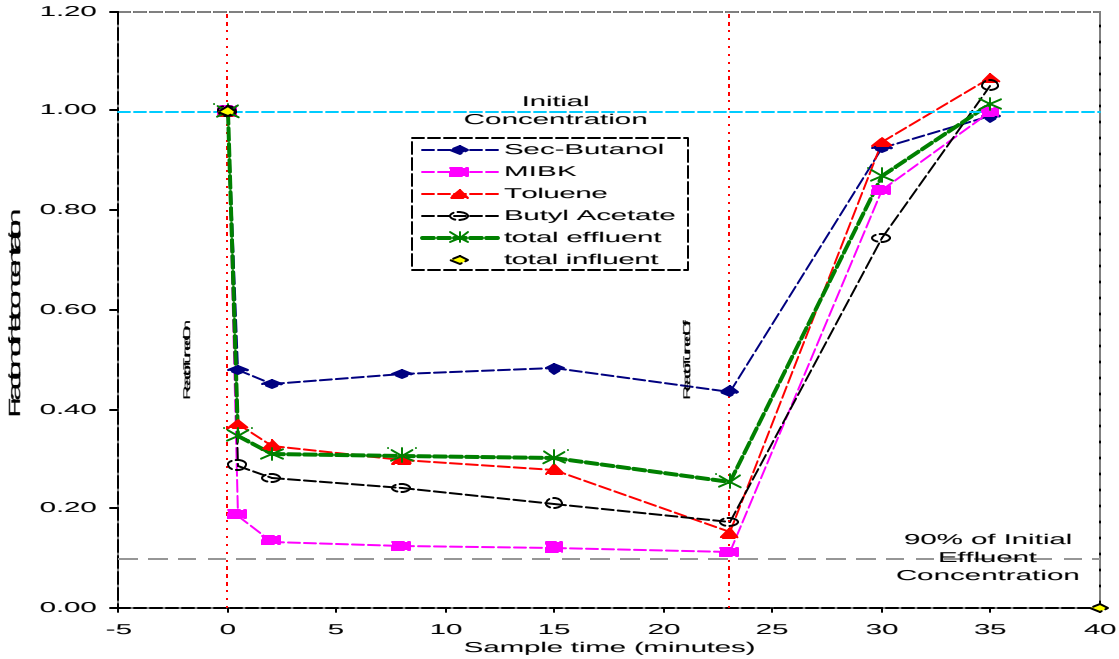

Figure 4.8 Destruction of VOCs in Single Dielectric Barrier Reactor at 15 kV, 300 Hz, and τ = 0.05 s

4.3 Effect of Voltage and Frequency on Destruction

Increase in voltage increased the overall destruction of the VOCs. This was expected, as increasing the voltage across the reactor increased the electric field in the annulus of the reactor, resulting in higher degree of ionization and higher overall destruction. Figure 4.9 shows the destruction of VOCs with increase in voltage. Voltage was increased from 60V primary (9.5 kV secondary) to 90V primary (15 kV secondary) in the 1 cm long single dielectric barrier reactor. The overall destruction of VOCs increased from 78 % to 91 %.

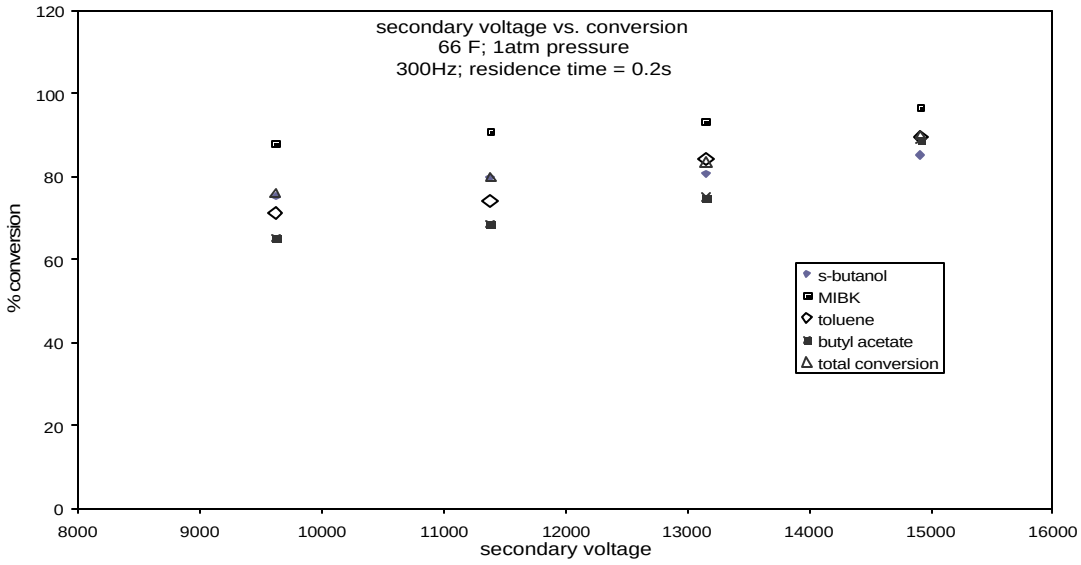

Figure 4.9 Applied Voltage vs. Overall Destruction of VOCs in the Single Dielectric Barrier Plasma Reactor at 300 Hz, and τ = 0.2 s

Increasing frequency increased overall VOC destruction. Frequency was measured at 200, 300 and 400 Hz at a residence time of 0.05 s. The results are summarized in Table 4.3. Due to the transformer's operational safety, frequency was maintained below 300 Hz for further plasma reactor studies.

TABLE 4.3
Effect of Frequency on Destruction of VOCs for applied voltage of 17 kV and τ = 0.05 s

Frequency (Hz)	**Overall VOC Destruction (%).**
200	56%
300	70%
400	83%

4.4 Effect of Humidity

Humidity increased the overall destruction in the reactor. The current across the reactor remained unchanged in the dry and the humid runs. Tests were performed at 35 – 40% and 70 – 80% relative humidity. Comparison of destruction with respect to relative humidity has been provided in Table 4.4. Figures 4.10 and 4.11 and show the VOC destruction plots for 35 – 40% and 70 – 80% relative humidity.

TABLE 4.4
Effect of Relative Humidity on Overall Destruction
of VOCs at 15 kV, 300 Hz, and τ = 0.2 s

Relative Humidity	**Overall VOC Destruction (%)**
0 %	91 %
30 – 45 %	96 %
70 – 80%	96 %

Figures 4.9 and 4.10 show that s-butanol had the higher percentage conversion in humid conditions (97%). This is possibly due the hydrophilic nature of s-butanol due to the polarization in the -C – OH bond. The polarization results in a strong nucleophilic site that can react with water and form a positively charged complex that can initiate further reactions [31].

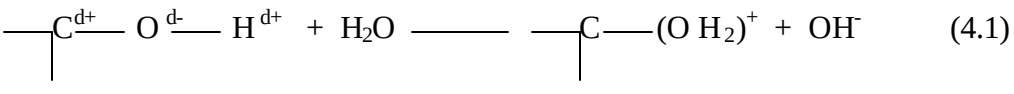

(4.1)

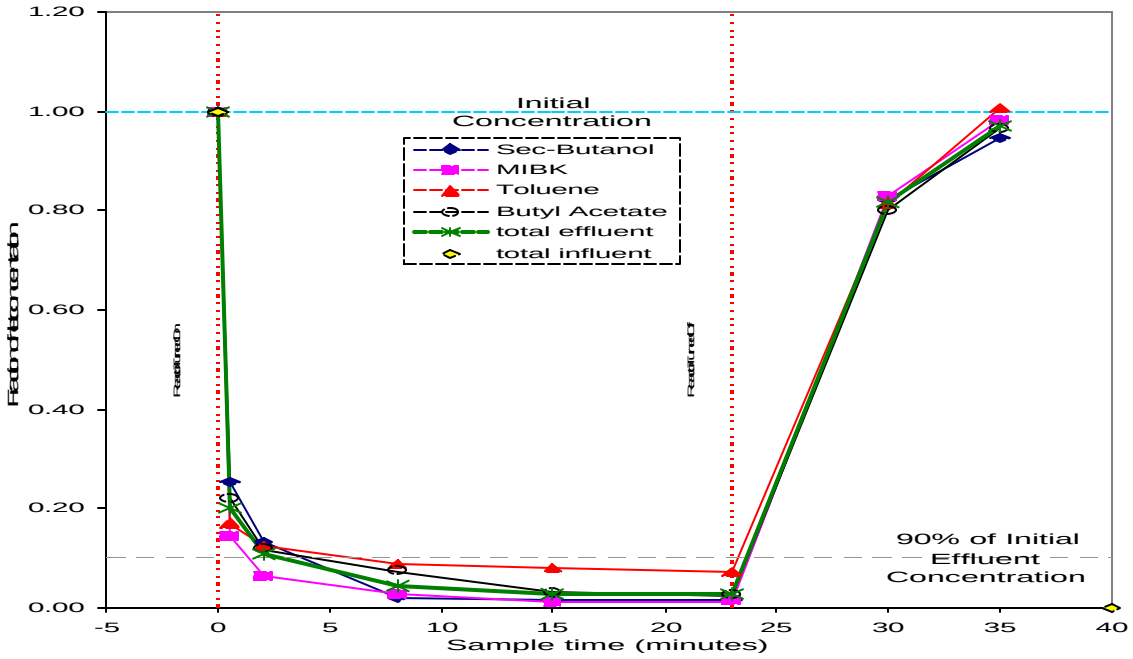

Figure 4.10 Destruction of VOCs at 12.4 kV, 300 Hz, 35 – 40 % relative humidity and $\tau = 0.2$ s

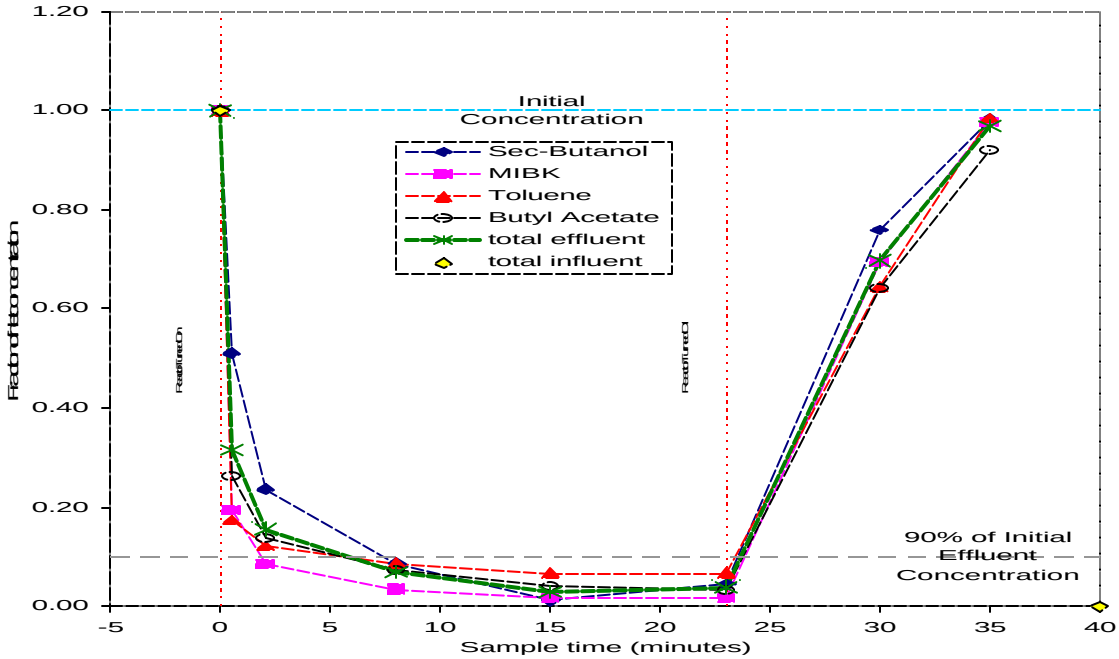

Figure 4.11 Destruction of VOCs at 12.4 kV, 300 Hz, 70 – 80 % relative humidity and $\tau = 0.2$ s

4.5 Reactor Configuration

Different reactor configurations were tested for overall percentage conversion of VOCs. Initial tests were conducted by increasing the reactor length from 1 cm to 10 cm. Table 4.5 summarizes the overall destruction with respect to the reactor length. This was followed by tests on reactor with 10 tubes in parallel. The outer electrode length of each tube was increased from 1 cm to 5 cm. The results are summarized in Table 4.6.

TABLE 4.5
Effect of Reactor Length on Destruction of VOCs at 15 kV, 300 Hz and τ = 0.2s

Reactor Length	Overall VOC Destruction (%)
1 cm	91 %
2 cm	96 %
4 cm	94 %
5 cm	93 %
10 cm	95 %

TABLE 4.6
Summary of Destruction with respect to Reactor Length in the 10 Tube Reactor at 15 kV, 300 Hz and τ = 0.2s

Reactor Length	Overall VOC Destruction (%)
1 cm	98 %
5 cm	90 %

Tests were also performed on a reactor with 1 inch outer diameter at different residence times. There was no VOC destruction in this reactor. The inlet and outlet concentrations remained the same even after the power source was switched on and set to different voltages. This is probably due to insufficient energy density in the reactor to initiate the oxidation reactions.

4.6 Ozone Concentration

The ozone concentration downstream of the reactor was determined using iodometric titration. Ozone concentration under dry conditions increased to a value of 496 ppm and stabilized at that concentration above applied voltage of 15000V. When relative humidity was 35 – 40%, the concentration of ozone increased to a value of 241 ppm for an applied voltage of 18500 V across the reactor, and then decreased to 208 ppm when the voltage was further increased to 20200 V. Figure 4.12 shows the comparative plot of downstream ozone concentration in 1 cm reactor in dry and humid conditions. The frequency was maintained at 300 Hz for the ozone tests and the residence time was 0.2 s. The ozone production trend was similar to those observed in literature [22, 23].

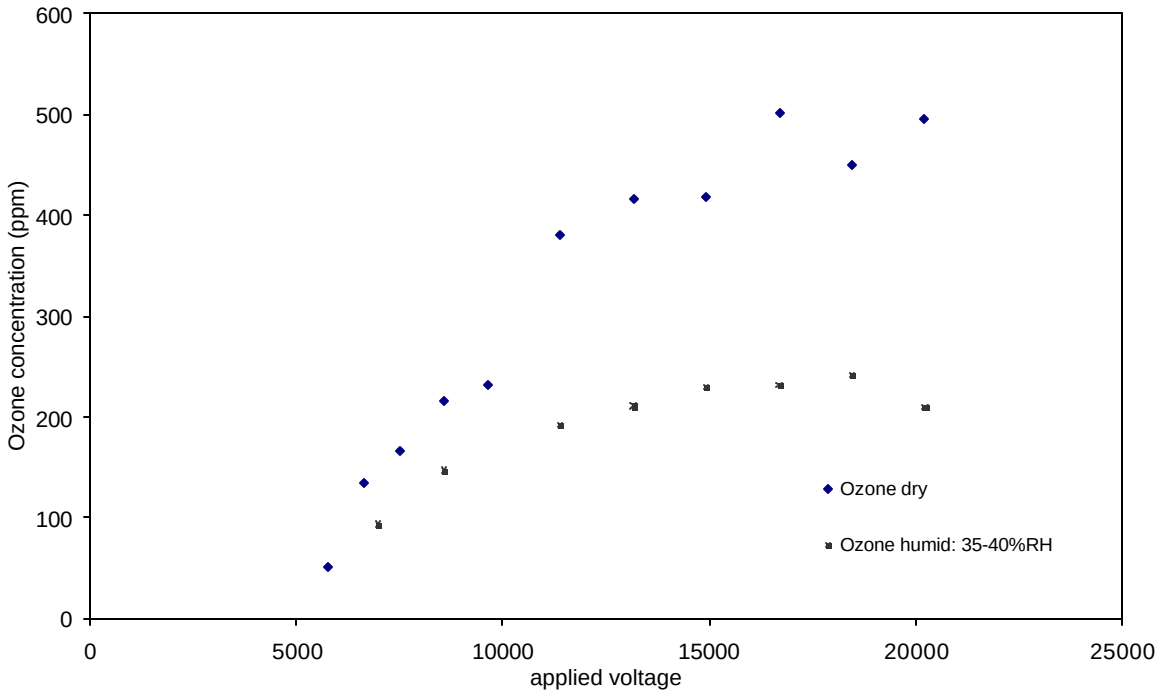

Figure 4.12 Downstream Ozone Concentration Comparisons in 1 cm reactor at 0% Relative Humidity (dry) and 35-40% Relative Humidity at 60 ^{o}F.

Ozone concentrations were also measured for different relative humidities, for two different applied voltages across the reactor. Ozone concentration was expected to be lower in humid air, as ozone dissociates in the presence of water molecule. For an applied voltage of 18500V, the concentration dropped from 241 ppm at 35% RH to 170 ppm at 85% RH. When a lower voltage of 11400 V was applied across the reactor, the concentration dropped from 191 ppm to 109 ppm with an increase in humidity from 35% RH to 85% RH. Figure 4.13 shows the variation in ozone concentration with humidity. The ozone production decreased with increase in humidity, and reached a stable value at high humidity. This is due to the high concentration of water molecules at high humidity, which would make ozone the limiting reagent in the dissociation process. Hence, a second degree curve serves as a good approximation of ozone production with respect to applied voltage.

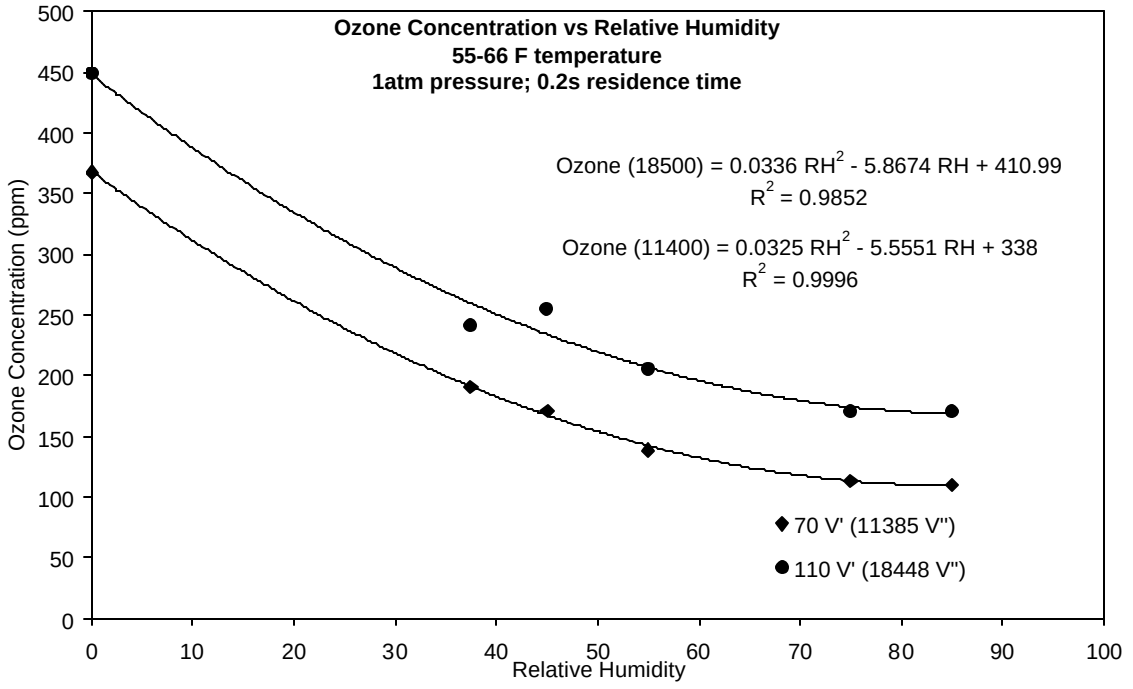

Figure 4.13 Downstream Ozone Concentration Variation with Relative Humidity at Different Applied Voltages, at 300 Hz and τ = 0.2 s.

Ozone concentration was also measured for 10 cm reactor in dry conditions and 35 – 40 % relative humidity. The results are summarized in Table 4.7. The ozone concentrations are average values of three different runs.

TABLE 4.7
Ozone Concentration in 10cm Reactor at 12.4 kV, 300 Hz, and τ = 0.2 s

Reactor Length	Humidity	Ozone Concentration (ppm)
10 cm	0 %	211
10 cm	35 – 40%	164

4.7 Electrical Measurements

Electrical measurements were obtained for reactors of different configurations. Power supplied to the reactor and the secondary currents were initially measured for single tube reactor with different lengths for constant secondary voltage and residence time. Secondary current remained unchanged in dry and humid conditions. Figure 4.14 shows the secondary current with respect to reactor length in dry and humid conditions. Secondary current had a linear fit with length of reactor. Power supplied to the reactor was also nearly equal in dry and humid conditions as power factor had similar values in both. The secondary power also had a linear fit. The results are shown in Figure 4.15.

For the same applied voltage, secondary current and power supply also increased with increasing number of tubes in the multiple tube reactor. Secondary current was measured for reactors with 1, 2, 4, 6, 8, and 10 tubes, each 5 cm in length. The plot had a linear fit. Figure 4.16 shows the secondary current with respect to the number of tubes in the reactor in dry condition. Secondary power also had a linear fit with number of tubes in the reactor, as shown in Figure 4.17. The average current drawn from the wall (I_w) was 4 amperes.

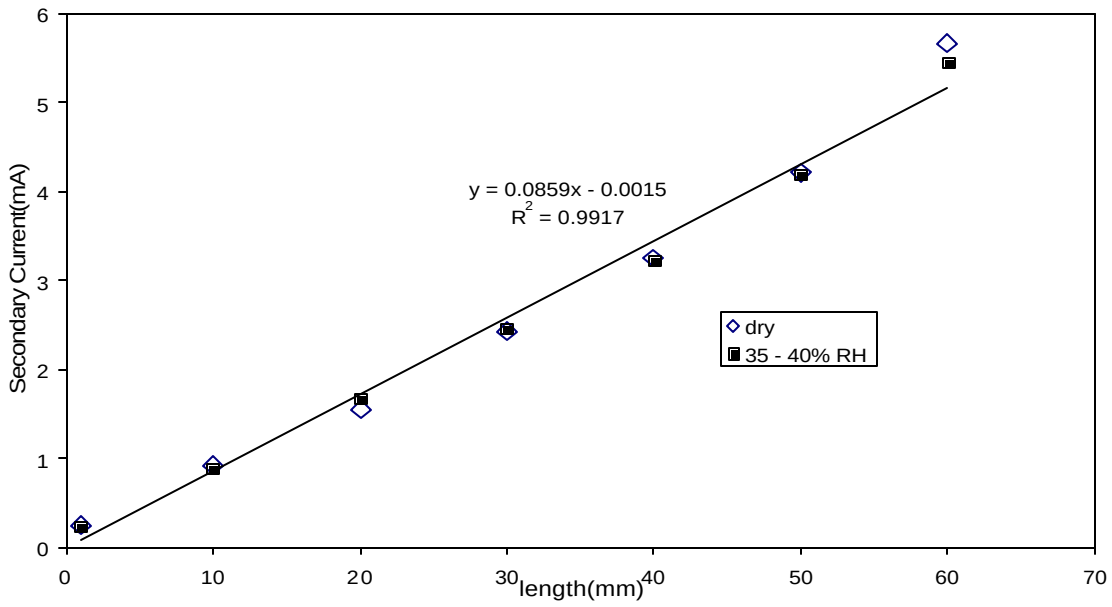

Figure 4.14 Secondary Current with respect to Reactor Length in Dry Condition and 35 – 40 % RH at 12.4 kV, 300 Hz, and τ = 0.2 s

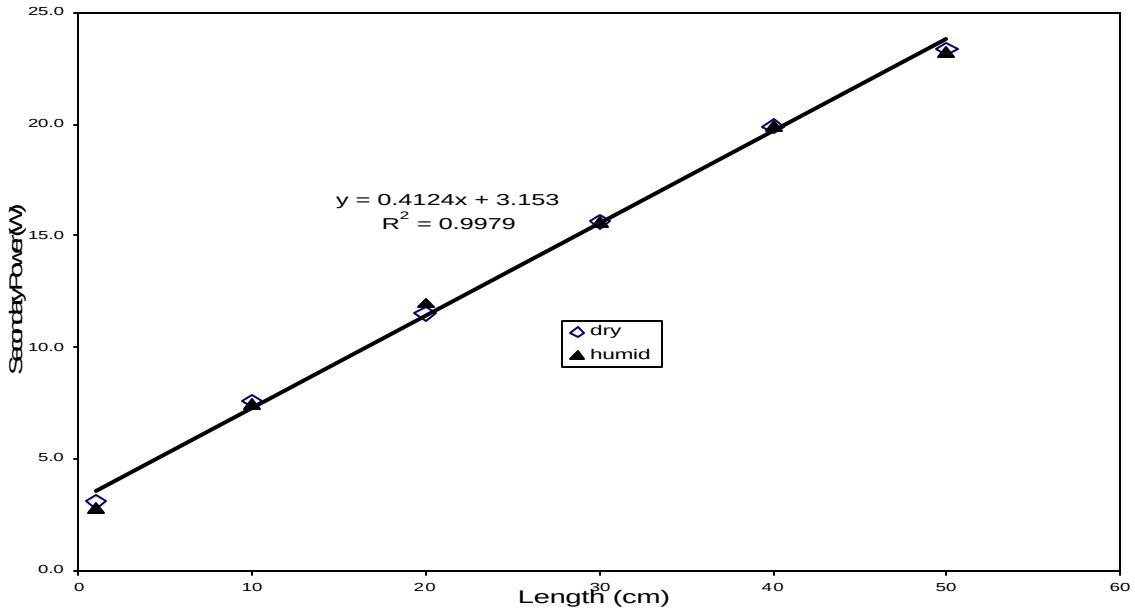

Figure 4.15 Power Supplied to Reactor with respect to Reactor Length in Dry Condition and 35 – 40 % RH at 12.4 kV, 300 Hz, and τ = 0.2 s

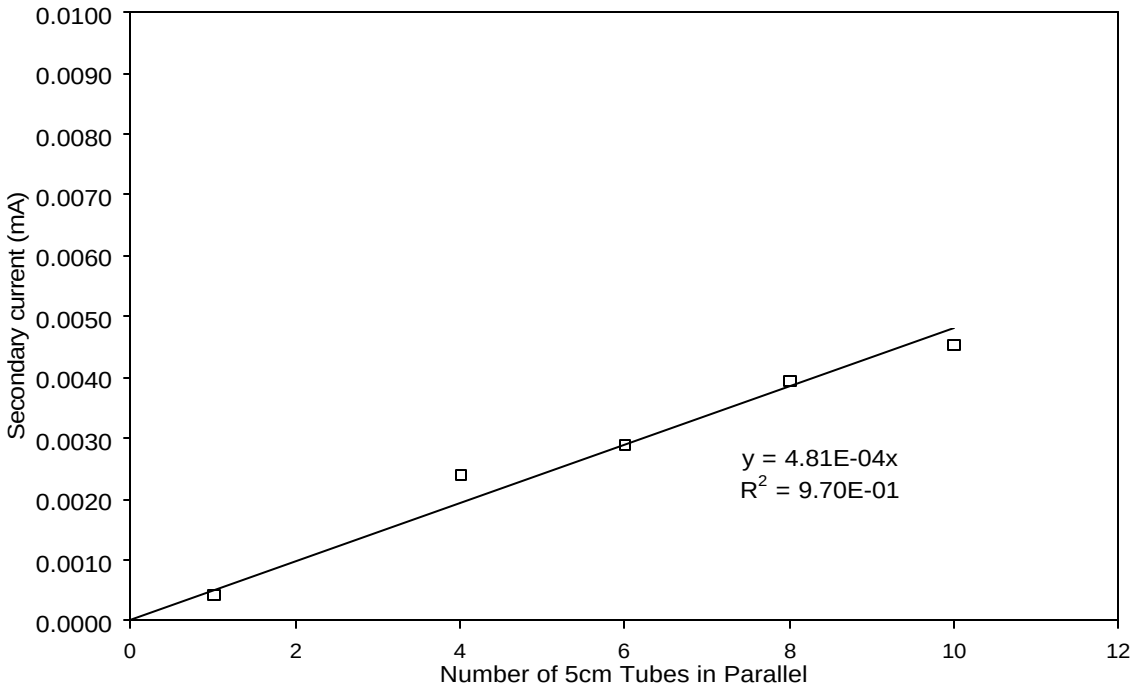

Figure 4.16 Secondary Current with respect to Number of 5 cm tubes in the Reactor at 12.4 kV, 300 Hz, and $\tau = 0.2$ s

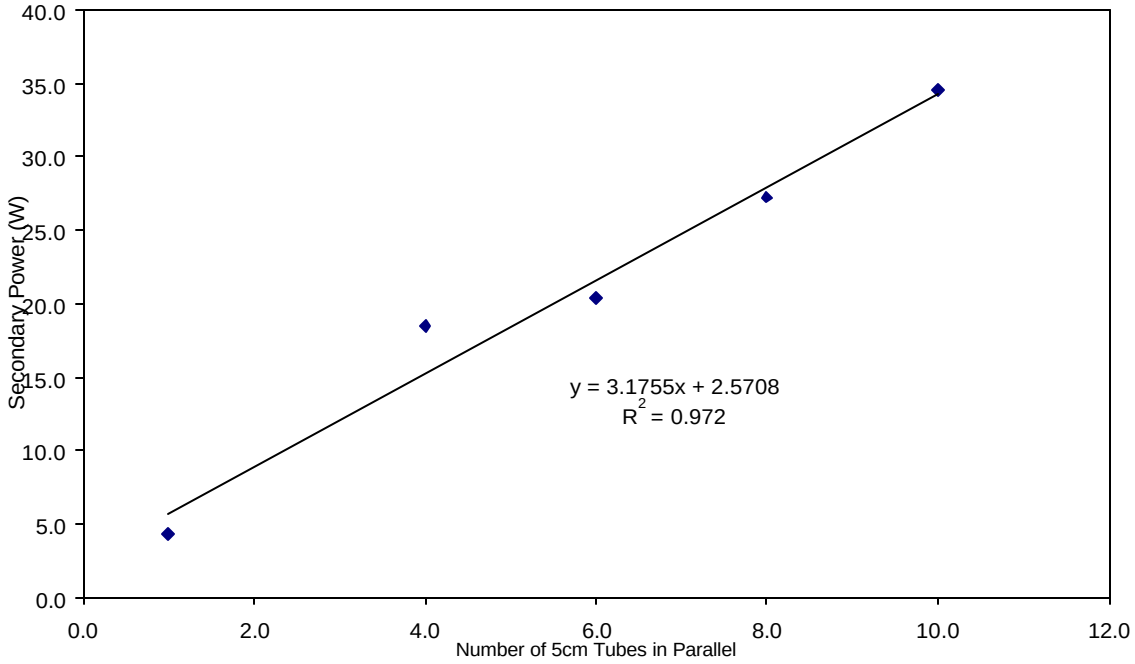

Figure 4.17 Secondary Power with respect to Number of 5 cm tubes in the Reactor at 12.4 kV, 300 Hz, and $\tau = 0.2$ s

On the primary side, for a constant applied voltage, the values of primary voltage, current and power first decreased and then increased with increase in reactor length. Similarly, when electrical measurements were made in multiple tube reactors, the primary voltage, current and primary power first increased with number of 5 cm tubes in parallel and then decreased. Residence time was maintained constant during the measurement of the electrical parameters. The values and trends of primary and secondary parameters were the same in both dry and humid conditions. Figures 4.18 through 4.20 show the variation in primary parameters for single tube reactor with respect to reactor length. As seen in the figures, the primary voltage, current and power supplied reached a minimum for reactor lengths between 30 and 40 cm. Hence, there is an optimum reactor length where the load on the power supply is minimal.

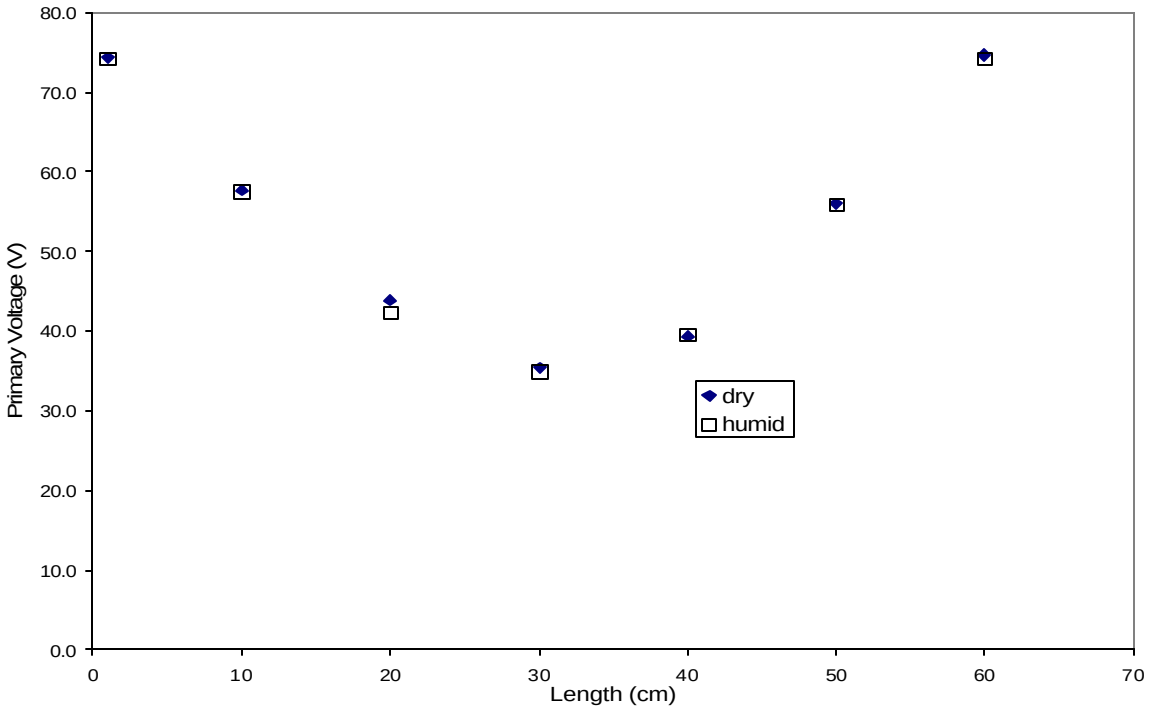

Figure 4.18 Primary Voltage with respect to Reactor Length in dry and humid condition (35 – 40 % RH)

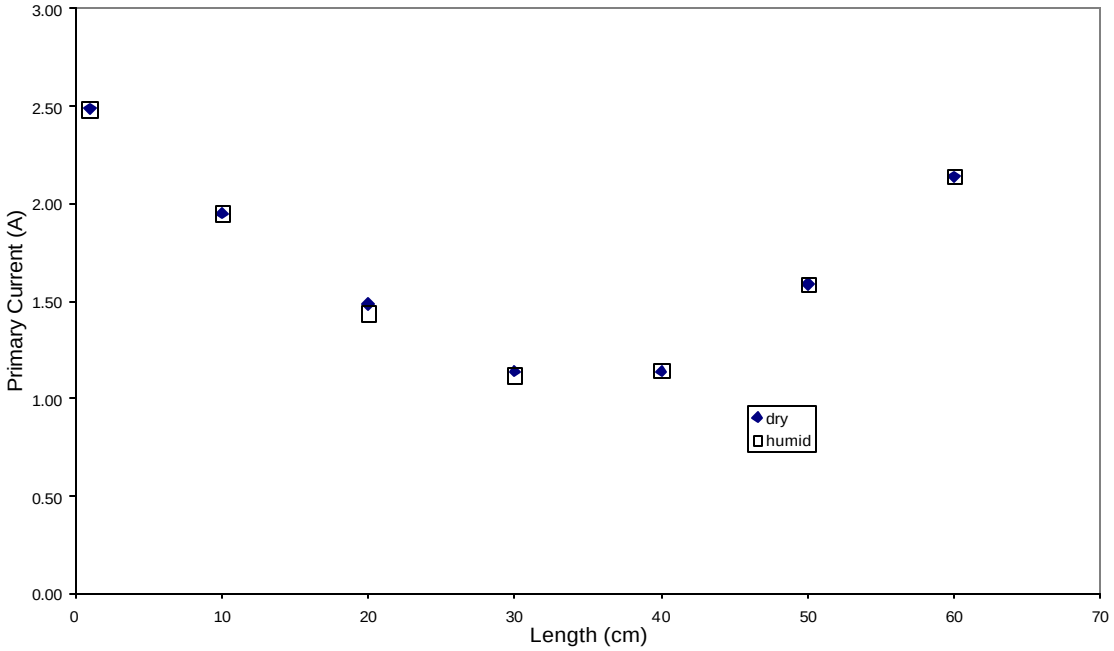

Figure 4.19 Primary Current with respect to Reactor Length in dry and humid condition (35 – 40 % RH)

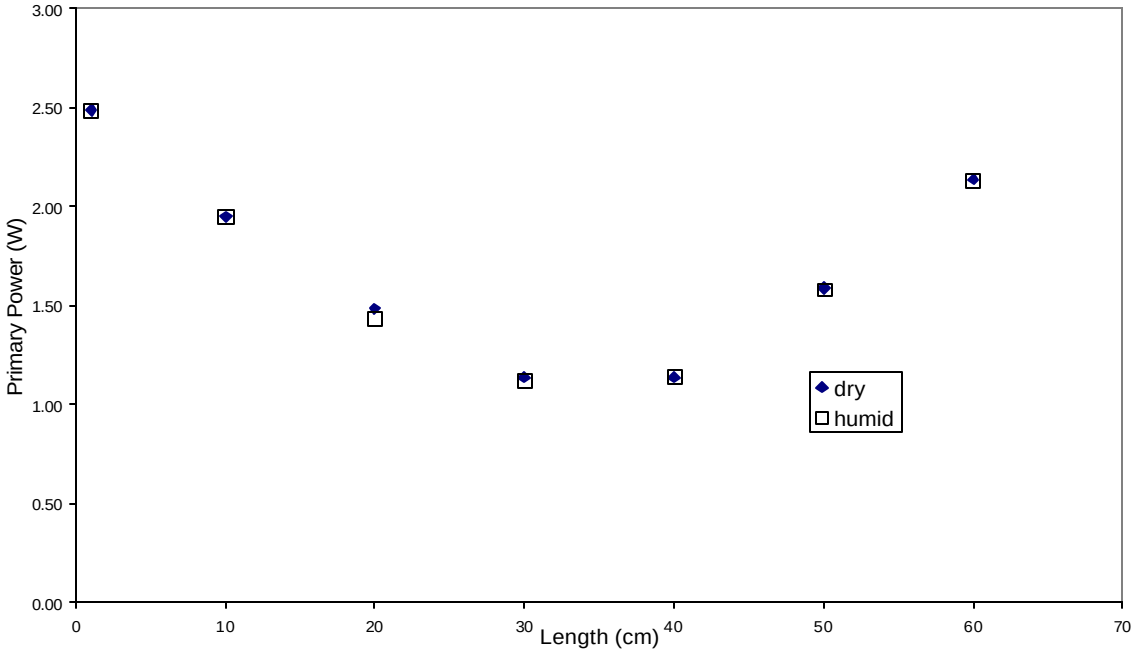

Figure 4.20 Primary Power with respect to Reactor Length in dry and humid condition (35 – 40 % RH)

Figures 2.21 through 2.23 show the variation in primary electrical parameters in the multiple reactors with respect to number of 5 cm reactors connected in parallel. The primary voltage, current and power supplied reached a minimum value between 4 and 6 reactors, suggesting that for an optimum number of reactors connected in parallel, the load on the power supply is minimal.

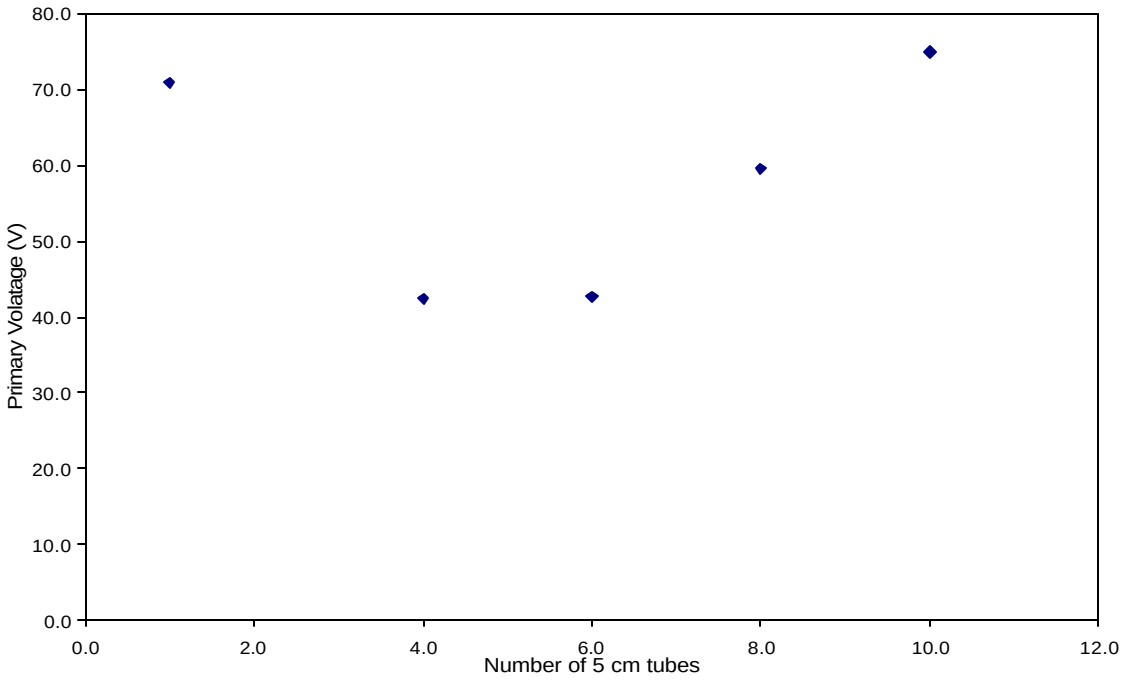

Figure 4.21 Primary Voltage with respect to Number of 5 cm tubes in Multiple Tube Reactor

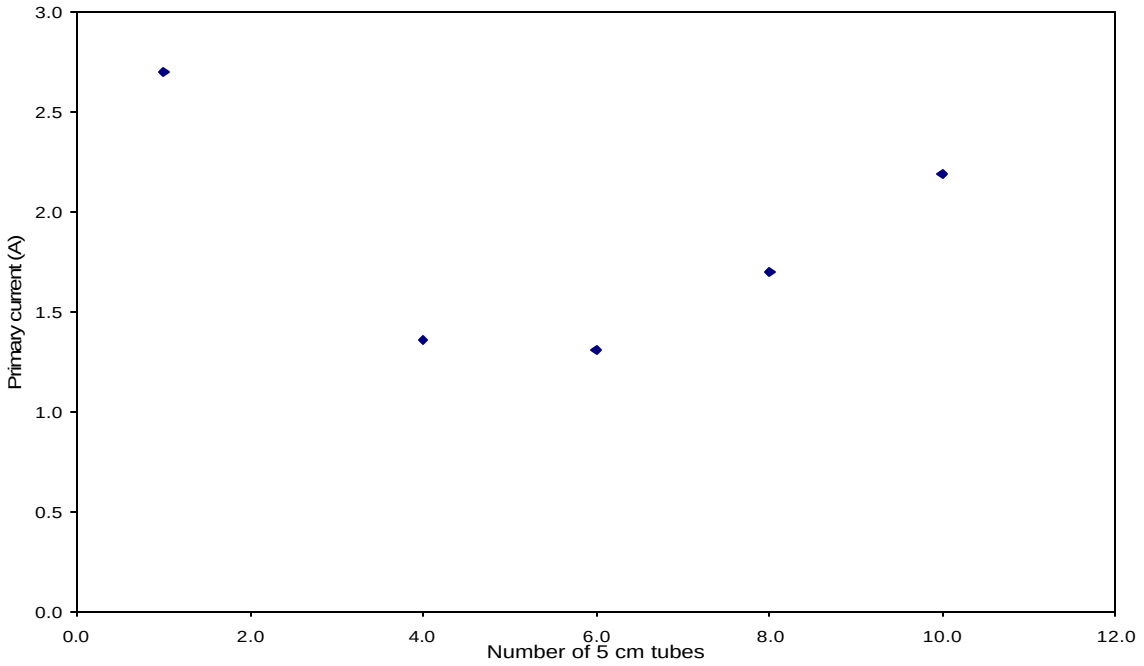

Figure 4.22 Primary Current with respect to Number of 5 cm tubes in Multiple Tube Reactor

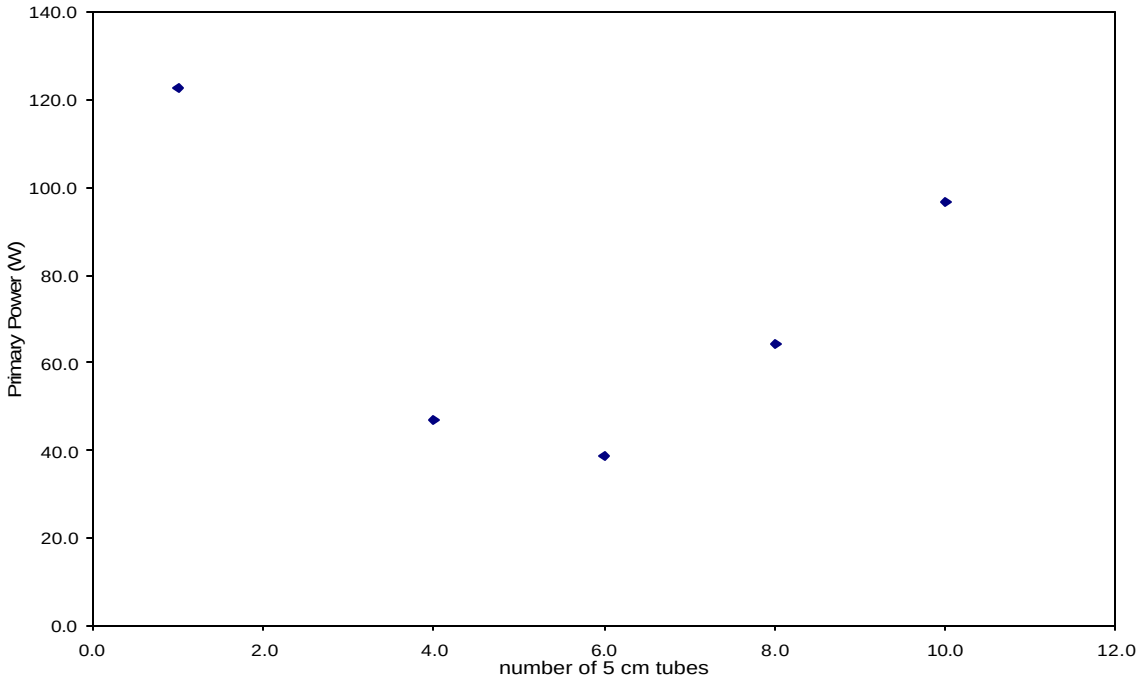

Figure 4.23 Primary Power with respect to Number of 5 cm tubes in Multiple Tube Reactor

4.8 Additional Observations

Though the temperature of the outer electrode of the 1 cm reactor did not increase significantly, the temperature of outer electrode of the 10 cm reactor increased with time. Temperature of downstream gas was obtained from the inline thermocouple reading. The average ambient temperature was 62.3 ^{o}F. The profile is shown in Figure 4.24. The figure shows the temperature of the downstream gas measured by the thermocouple. The temperature of the gas increased with time due to the increase in temperature of the outer electrode of the reactor and the resultant heat transfer to the gas.

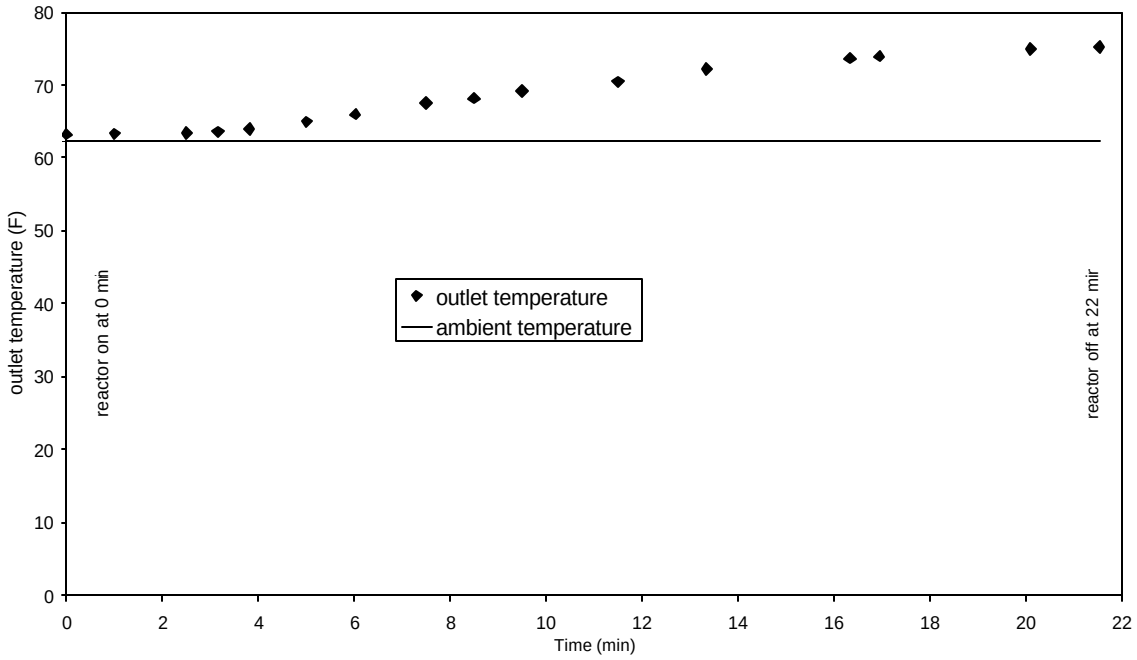

Figure 4.24. Temperature Profile of Downstream Gas in the 10 cm Reactor.

The glow in the plasma reactor extended beyond the confines of inner and outer electrodes in both directions up to 1 or 2 cm depending on the length of the reactor. This

weak end-effect was due to the electric potential developed between air and the inner electrode, as the inner electrode was not covered with a dielectric.

On the whole, the plasma reactor performed satisfactorily. Quartz had enough electrical and mechanical strength to act as the dielectric and material of construction of the reactor. Though one transformer broke down due to operational frequency reaching above 400 Hz, the replacement luminous tube transformer performed without any major problems when frequency was maintained below 300 Hz. Though overall the experiments provided good insight into destruction trends of VOCs in different reactor configurations and scale up requirements, there is still scope for further improvements and more advanced studies.

CHAPTER 5

EXPERIMENTAL RECOMMENDATIONS

As recommended by Holland [32], an electrical circuit was designed to obtain secondary parameters after modifying the design specified by Feng et al. [29]. But the following have to be implemented to obtain more detailed information to model VOC oxidation mechanism and scale up design:

- The use of a GC/MS would provide information about important intermediates in the oxidation mechanism of the VOCs. Also, it can be used to determine the difference in the kinetics of oxidation, if any, in dry and humid conditions.
- To prepare the influent VOC standard, the injection method could be improved. The liquid sample should be injected in a vessel with a larger volume so there is more residence time for mixing and obtaining an even concentration in the air. Or, alternately, the liquid mixture can be injected in a pressurized cylinder containing dry or humid air, as required. This method has been suggested by numerous researchers.
- The current setup has means of measuring temperature. But for detailed modeling, a pressure and temperature control system should be installed in the plasma system so that data are available to model the annular tube reactor as a plug flow or a laminar flow reactor. VOC oxidation is affected by both temperature and pressure. Hence, scale up modeling can be made more detailed with the variables known.

- Studies have to be conducted with the use of catalysts in the plasma reactor. Barium titanate has been used successfully in studies conducted by Yamamoto et al. [19]. Catalysts used in catalytic processes can be tried in the plasma reactor for possible improvements in oxidation efficiency.

REFERENCES

1. EPA (1996), Federal Facilities Sector Notebook: A Profile of Federal Facilities, 300 – B – 96 – 003.

2. Nunez, C. M., Ramsey G. H., Ponder, W. H., Abbot, J. H., Hamel, L. E., and Kariher, P. H. (1993). "Corona Destruction: An Innovative Control Technology for VOCs and Air Toxics." Air and Waste **43**(2): 242 - 247.

3. Yan, K., Hui, H., Cui, M., Miao, J., Xiaoli, W., Bao, C., and Li, R. (1998). "Corona Induced Non-Thermal Plasmas: Fundamental Study and Industrial Applications." Journal of Electrostatics **44**: 17 - 39.

4. EPA (1994), Indoor Air Pollution: An Introduction for Health Professionals, 402-R-94-007.

5. EPA (2003), Ozone: Good Up High Bad Nearby, EPA-451/K-03-001.

6. OSHA (1991). Chemical Information Manual, OSHA Instruction CPL. 2-2.43A.

7. Piatt, M. A. (1988). "Methane Destruction in an Alternating Current Plasma Reactor" – M.S. Thesis. Chemical Engineering. Stillwater, Oklahoma State University.

8. Desai, V. (1992). "Destruction of Hydrogen Sulphide in an Alternating Current, Frequency Tuned Plasma Reactor" – M.S. Thesis. Chemical Engineering. Stillwater, Oklahoma State University.

9. Siddhu, G. S. (1995). "Production and Destruction of Nitric Oxides in Alternating Current Plasma Reactor" – M.S. Thesis. Chemical Engineering. Stillwater, Oklahoma State University.

10. Magunta, S. R. (1995). "Studies on Destruction of Hydrogen Sulfide Mixed with Carbon Dioxide in an Alternating Current Plasma Arc Reactor" – M.S. Thesis. Chemical Engineering. Stillwater, Oklahoma State University.

11. Hurst, M. C. (1993). "Destruction of Carbon Tetrachloride in an Alternating Current Plasma Reactor" – M.S Thesis. Environmental Engineering. Stillwater, Oklahoma.

12. Parker, G. W. (1996). "Conceptual Design of an Industrially Applicable Plasma Reactor" – M.S. Thesis. Chemical Engineering. Stillwater, Oklahoma State University.

13. Lytle, P. H. (1998). “Destruction of Nitrogen Oxides Using a Dielectric Barrier Discharge Plasma Reactor” – M.S. Thesis. Environmental Engineering. Stillwater, Oklahoma State University.

14. Eliasson, B., and Kogelschatz, U. (1991). "Nonequilibrium Volume Plasma Processing." IEEE Transactions on Plasma Science **19**(6): 1063 - 1077.

15. Liu, C. (2002). "Catalyst preparation using plasma technologies." Catalysis Today **72**: 173 - 184.

16. Cal, M. P. (2001). "Destruction of Benzene with Non Thermal Plasma in Dielectric Barrier Discharge Reactors." Environmental Progress **20**: 151-156.

17. Eliasson, B. (1991). "Modeling and Application of Silent Discharge Plasmas." IEEE Transactions on Plasma Science **19**(2): 309 - 323.

18. Yan, K., van Heesh, E. J. M., Pemen, A. J. M., and Huijbrechts, P. A. H. J. (2001). "From Chemical Kinetics to Streamer Corona Reactor and Voltage Pulse Generator." Plasma Chemistry and Plasma Processing **21**(1): 107 - 137.

19. Yamamoto, T., Ramanathan, K., Lawless, P. A., Ensor, D. S., Newsome, J. R., Plaks, N., and Ramsey, G.H. (1992). "Control of Volatile Organic Compounds by an ac Energized Ferroelectric Pellet Reactor and a Pulsed Corona Reactor." IEEE Transactions on Industry Applications **28**(3): 528 - 534.

20. Halliday, D., Resnick, R., and Walker, J. (1996). Fundamentals of Physics. John Wiley and Sons.

21. Roland, U., Holzer, F., and Kopinke, F. -D. (2002). "Improved Oxidation of Air Pollutants in a Non-Thermal Plasma." Catalysis Today **73**: 315 - 323.

22. Yamamoto, T. (1997). "VOC Decomposition by Nonthermal Plasma Processing - A New Approach." Journal of Electrostatics **42**: 227 - 238.

23. Oda, T. (2003). "Non-thermal Plasma Processing for Environmental Protection: Decomposition of Dilute VOCs in Air." Journal of Electrostatics **57**: 293 - 311.

24. Evans, D., Rosocha, L. A., Anderson, G. K., Coogan, J. J., and Kushner, M. J. (1993). "Plasma Remediation of Trichloroethylene in Silent Discharge Plasmas." Journal of Applied Physics **74**(9): 5378 - 5386.

25. Rosocha, L. A., Coogan, J. J., and Kang, M. (1994). Use of Silent Electric Discharges for Environmental Remediation. IEEE International Conference on Plasma Science, New Jersey.

26. Gentile, A. C., and Kushner, M. J. (1995). "Plasma Remediation of Perchloroethylene in Humid Gas Streams." Journal of Applied Physics **78**(5): 2977 - 2980.

27. Pasquiers, S., Cormier, M., and Motret, O. (2002). Atmospheric Pollutant Removal by Non-Thermal Plasmas: Basic Data Needs for Understanding and Optimization of the Process. Atomic and Molecular Data and Their Application: 3rd Int'l. Conf. American Institute of Physics.

28. Holland, G. D., Veenstra, J. N., Johannes, A. H., Foutch, G, L., and Hall, F. (2004). Reduction of VOC Emissions from Paint-Booth Operations Using Dielectric Barrier Discharge. 30th Environmental and Energy Symposium & Exhibition, San Diego.

29. Feng, R., Castle, G. S. P., and Jayaram, S. (1998). "Automated System for Power Measurement in the Silent Discharge." IEEE Transactions on Industry Applications **34**(3): 563 - 570.

30. APHA, AWWA, and WCPF (1975). Iodometric Determination of Ozone. Standard Methods for the Examination of Water and Waste Water, 14th edition.

31. Morrison, R. T., and Boyd, R.N. (1987). Organic Chemistry. Boston, Allyn and Bacon.

32. Holland, G. D. (2002). "Reaction of Methane in a Dielectric Barrier Discharge Plasma Reactor" – PhD Thesis. Chemical Engineering. Stillwater, Oklahoma State University.

APPENDIX A

MASS FLOW CALIBRATION

A.1. Calibration of Flow Control Equipments

The Mass Flow Controllers, labeled M1 and M3, were calibrated with an Altech Digital Mass Flow Meter. Figure A.1 shows the calibration of M1. The range of M1 was 6.2 – 48.5 sccm. The flow rate of air through M1 had a linear fit with the Digital Mass Flow Meter reading.

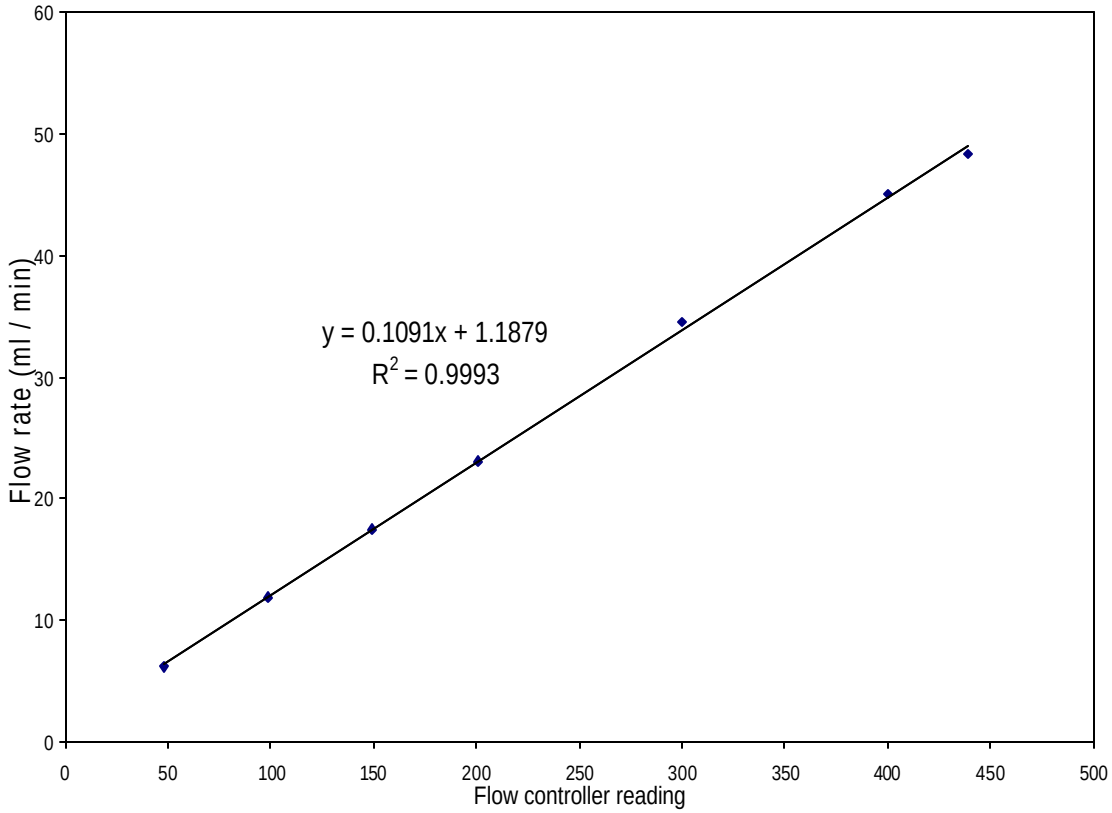

Figure A.1. Calibration of Flow Controller M1

Figure A.2. shows the calibration of the Mass Flow Controller M3. The range of the M3 was was 48 – 745 sccm. The flow rate of air through M3 also had a linear fit with respect to the Digital Mass Flow Meter reading.

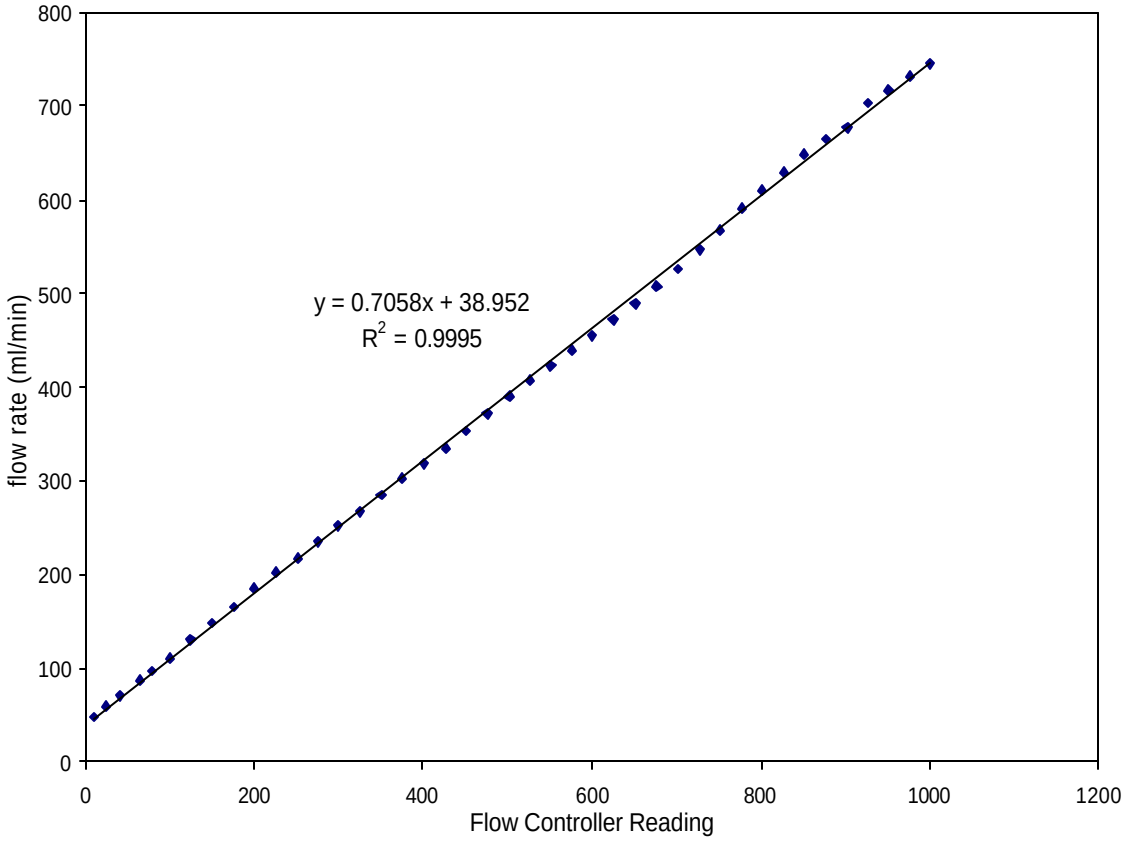

Figure A.2. Calibration of Flow Controller M2

The calibration of the rotameter is shown in Figure A.3. The flow rate of air was measured with respect to the height of the top of the ball in the rotameter. Calibration of the rotameter was done with a wet flow meter. The flow rate of air had a linear fit with respect to the height of the ball. The rotameter was calibrated from 832 – 13000 sccm.

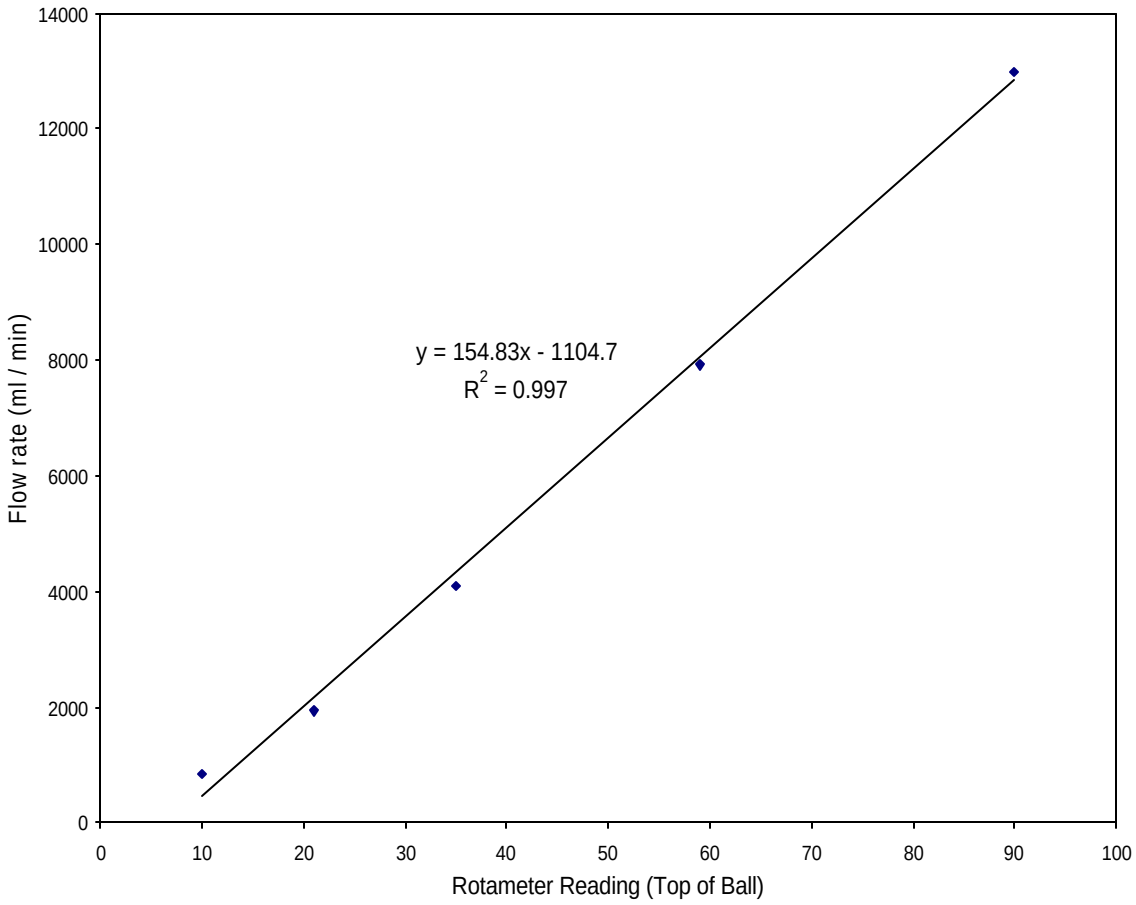

Figure A.3. Calibration of Rotameter

APPENDIX B

CALCULATION OF LIQUID VOC RATIO AND LIQUID INJECTION RATE

B.1. Calculation of VOC Ratio in Liquid Mixture

The emission levels of s-butanol, methyl isobutyl ketone, toluene and butyl acetate have been listed in Table 1.1. The mass ratios of the four VOCs were used to calculate their volumetric ratio in the liquid mixture.

Volumetric ratio for the liquid mixture was obtained by dividing the mass ratio of the VOCs with their respective densities and rearranging. Loss of mixture volume was assumed negligible while preparing the liquid VOC mixture.

Molar ratio was obtained by dividing the mass ratio of the VOCs with their respective molar masses and rearranging. Their densities and molar masses were obtained from the manufacturers.

	s-butanol	:	methyl isobutyl ketone	:	toluene	:	butyl acetate
	(0.802 g / ml)		(0.801 g / ml)		(0.867 g / ml)		(0.882 g / ml)
	(74.12 g / mole)		(100.16 g / mole)		(92.14 g / mole)		(116.16 g / mole)
Mass ratio:	0.057		0.045		0.012		0.049
Volume ratio:	5.07		4.00		1.00		3.93
Molar ratio:	5.92		3.46		1.00		3.23

B.2. Calculation of Injection Rate of VOCs

Injection rate was calculated to obtain a total VOC concentration of 100 ppm. An example of injection rate calculation is given below for air flow rate of 141 ml / min:

$$\text{Air flow rate} = 141 \ \frac{ml}{\text{min}}$$

$$= \left(\frac{141}{22400}\right) \frac{mole}{\text{min}} \ \text{(Assuming ideal gas at STP)}$$

$$= 0.0063 \ \frac{mole}{\text{min}}$$

Hence, total VOC injection rate = $6.30 \times 10^{-7} \frac{mole}{\min}$ (To obtain 100 ppm in air)

Injection rate of toluene = $0.46 \times 10^{-7} \frac{mole}{\min}$ (From molar ratio of VOCs)

$$= 0.46 \times 10^{-7} \frac{mole}{\min} \times 92.14 \frac{g}{mole} \times \frac{1}{0.867} \frac{ml}{g}$$

$$= 49 \times 10^{-7} \frac{ml}{\min}$$

Total VOC injection rate = $6.9 \times 10^{-5} \frac{ml}{\min}$ (From volume ratio of VOCs)

$$= 0.07 \frac{ml}{\min}$$

APPENDIX C

GAS CHROMATOGRAPH CALIBRATION FOR VOCs

C.1. Calibration Curves of VOCs

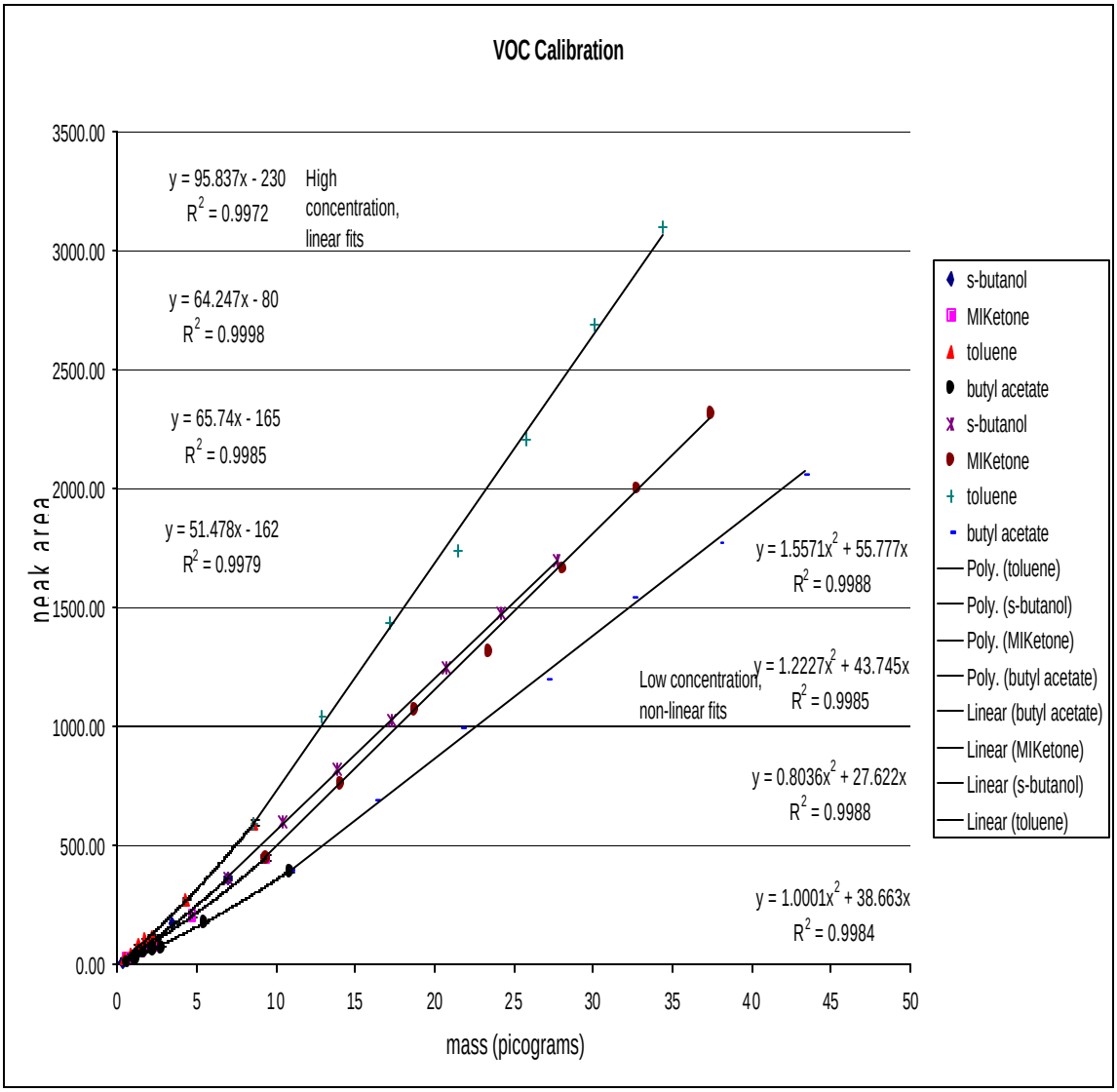

Figure C.1. Calibration Curves of VOCs for Low and High Concentrations.

The GC was calibrated for the VOCs using a standard mixture of 100 ppm each of s-butanol, toluene, methyl isobutyl ketone and butyl acetate. Figure C.1 shown in the previous page shows the calibration curve. The area of the peak obtained for each VOC in the GC output corresponded to the mass of compound in the injection.

For lower injection volumes (0.01 ml to 0.1 ml), a non – linear fit was obtained for the area of the peaks with respect to the mass of the VOCs present in the sample. For higher injection volumes (0.1 ml to 0.8 ml), the peak areas had a linear fit with respect to the mass of VOCs.

APPENDIX D

DESTRUCTION DATA

The following sections show the destruction data for all the destruction runs that were discussed in Chapter 4. Table D.1. shows the type of data presented in each section.

TABLE D.1
Type of Data Presented in Each Section of Appendix D

Section	Type of Data Presented
D.1	VOC Destruction in Single and Double Dielectric Barrier Reactors
D.2	VOC Destruction Data for Various Residence Times
D.3	VOC Destruction Data for Various Applied Voltages
D.4	VOC Destruction Data for Humid Runs
D.5	VOC Destruction Data for Different Reactor Lengths
D.6	VOC Destruction Data for Multiple Tube Reactors

Part (a) of each of the following tables shows the concentration data, in which the influent and effluent concentrations for each compound and overall VOCs (in ppm) are tabulated for the samples collected at different times after the reactor was switched on.

Part (b) of each of the following tables shows the normalized data, in which the fraction of the original inlet concentration has been shown for each VOC and total effluent at different times after the reactor was switched on.

D.1. Destruction Data for Single Dielectric and Double Dielectric Barrier Reactors

TABLE D.2
Destruction Data for Double Dielectric Barrier Reactor

(a) Concentration Data (in ppm)

Sampling Time (min)	0	0.5	2	8	15	23	30	35
Sec-butanol	29.5	20.0	7.8	6.5	3.5	1.8	25.3	29.3
MIBK	20.5	5.2	4.9	4.3	4.1	1.8	17.8	20.1
Toluene	14.4	12.5	8.1	5.7	3.7	3.3	10.7	13.5
Butyl Acetate	11.7	7.6	4.3	2.7	2.0	1.1	11.4	12.6
Total Effluent	76.1	45.4	25.2	19.2	13.3	8.1	65.2	75.5

(b) Normalized Data (Fraction of Inlet Concentration)

Sampling Time (min)	0	0.5	2	8	15	23	30	35
Sec-Butanol	1.00	0.68	0.26	0.22	0.12	0.06	0.86	0.99
MIBK	1.00	0.25	0.24	0.21	0.20	0.09	0.87	0.98
Toluene	1.00	0.87	0.56	0.39	0.26	0.23	0.74	0.94
Butyl Acetate	1.00	0.65	0.37	0.23	0.17	0.09	0.98	1.08
Total Effluent	**1.00**	**0.60**	**0.33**	**0.25**	**0.17**	**0.11**	**0.86**	**0.99**

TABLE D.3
Destruction Data for Single Dielectric Barrier Reactor

(a) Concentration Data (in ppm)

Sampling Time (min)	0	0.5	2	8	15	23	30	35
Sec-Butanol	31.6	8.9	4.5	3.2	2.4	1.1	29.2	31.2
MIBK	22.7	8.9	2.7	1.8	2.3	1.1	19.7	22.2
Toluene	14.9	6.0	2.1	2.1	1.7	0.9	12.0	14.4
Butyl Acetate	13.1	7.2	2.9	2.2	2.3	1.3	11.8	12.8
Total Effluent	**82.3**	**31.0**	**12.2**	**9.3**	**8.8**	**4.4**	**72.8**	**80.6**

(b) Normalized Data (Fraction of Inlet Concentration)

Sampling Time (min)	0	0.5	2	8	15	23	30	35
Sec-Butanol	1.00	0.28	0.14	0.10	0.08	0.04	0.93	0.99
MIBK	1.00	0.39	0.12	0.08	0.10	0.05	0.87	0.97
Toluene	1.00	0.40	0.14	0.14	0.11	0.06	0.81	0.96
Butyl Acetate	1.00	0.55	0.22	0.17	0.17	0.10	0.90	0.97
Total Effluent	**1.00**	**0.38**	**0.15**	**0.11**	**0.11**	**0.05**	**0.88**	**0.98**

D.2. Destruction Data for Various Residence Times

TABLE D.4
Destruction Data for $\tau = 0.6$ s

(a) Concentration Data (in ppm)

Sampling Time (min)	0	0.5	2	8	15	23	30	35
Sec-Butanol	30.4	11.8	10.1	6.5	6.5	9.6	27.0	31.7
MIBK	20.0	11.8	7.2	2.6	2.6	2.7	17.0	20.3
Toluene	13.2	11.3	5.7	2.0	2.0	2.1	11.0	13.0
Butyl Acetate	12.7	10.8	8.0	3.1	3.1	2.8	10.4	11.9
Total Effluent	**76.2**	**45.8**	**31.1**	**14.2**	**14.2**	**17.2**	**65.4**	**76.9**

(b) Normalized Data (Fraction of Inlet Concentration)

Sampling Time (min)	0	0.5	2	8	15	23	30	35
Sec-Butanol	1.00	0.39	0.33	0.22	0.22	0.32	0.89	1.04
MIBK	1.00	0.59	0.36	0.13	0.13	0.14	0.85	1.02
Toluene	1.00	0.86	0.43	0.15	0.15	0.16	0.83	0.98
Butyl Acetate	1.00	0.85	0.63	0.25	0.25	0.22	0.82	0.94
Total Effluent	**1.00**	**0.60**	**0.41**	**0.19**	**0.19**	**0.23**	**0.86**	**1.01**

TABLE D.5
Destruction Data for $\tau = 0.4$ s

(a) Concentration Data (in ppm)

Sampling Time (min)	0	0.5	2	8	15	23	30	35
Sec-Butanol	31.4	10.3	8.2	7.3	7.3	5.2	30.2	31.3
MIBK	20.6	3.5	1.6	1.0	1.0	1.0	21.1	22.2
Toluene	13.8	4.1	3.0	2.3	2.3	1.8	13.6	13.7
Butyl Acetate	13.4	4.5	2.2	1.3	1.3	1.0	12.7	14.6
Total Effluent	**79.2**	**22.5**	**15.0**	**11.9**	**11.9**	**9.0**	**77.6**	**81.8**

(b) Normalized Data (Fraction of Inlet Concentration)

Sampling Time (min)	0	0.5	2	8	15	23	30	35
Sec-Butanol	1.00	0.33	0.26	0.23	0.23	0.17	0.96	1.00
MIBK	1.00	0.17	0.08	0.05	0.05	0.05	1.03	1.08
Toluene	1.00	0.30	0.22	0.17	0.17	0.13	0.98	0.99
Butyl Acetate	1.00	0.33	0.17	0.10	0.10	0.07	0.95	1.09
Total Effluent	**1.00**	**0.28**	**0.19**	**0.15**	**0.15**	**0.11**	**0.98**	**1.03**

TABLE D.6
Destruction Data for $\tau = 0.2$ s

(a) Concentration Data (in ppm)

Sampling Time (min)	**0**	**0.5**	**2**	**8**	**15**	**23**	**30**	**35**
Sec-Butanol	29.1	6.2	3.6	1.6	1.6	0.5	23.8	31.3
MIBK	20.2	3.6	1.6	0.7	0.7	0.6	16.6	22.2
Toluene	12.4	5.8	3.2	1.7	2.7	1.4	9.7	13.7
Butyl Acetate	13.3	3.5	2.1	1.0	0.9	0.7	11.5	14.6
Total Effluent	**75.1**	**19.0**	**10.5**	**5.0**	**6.0**	**3.2**	**61.6**	**81.8**

(b) Normalized Data (Fraction of Inlet Concentration)

Sampling Time (min)	**0**	**0.5**	**2**	**8**	**15**	**23**	**30**	**35**
Sec-Butanol	1.00	0.21	0.12	0.05	0.05	0.02	0.82	1.08
MIBK	1.00	0.18	0.08	0.04	0.04	0.03	0.82	1.10
Toluene	1.00	0.47	0.26	0.14	0.22	0.11	0.78	1.10
Butyl Acetate	1.00	0.26	0.16	0.08	0.07	0.05	0.87	1.10
Total Effluent	**1.00**	**0.25**	**0.14**	**0.07**	**0.08**	**0.04**	**0.82**	**1.09**

TABLE D.7
Destruction Data for $\tau = 0.1$ s

(a) Concentration Data (in ppm)

Sampling Time (min)	**0**	**0.5**	**2**	**8**	**15**	**23**	**30**	**35**
Sec-Butanol	31.8	12.8	11.8	11.7	10.3	11.9	27.9	29.7
MIBK	21.8	1.9	0.7	0.0	0.0	0.0	19.6	21.1
Toluene	13.9	3.5	2.3	1.7	1.5	1.8	12.7	13.2
Butyl Acetate	14.1	2.3	1.4	1.0	0.7	0.8	13.2	13.5
Total Effluent	**81.6**	**20.5**	**16.1**	**14.4**	**12.5**	**14.4**	**73.3**	**77.6**

(b) Normalized Data (Fraction of Inlet Concentration)

Sampling Time (min)	**0**	**0.5**	**2**	**8**	**15**	**23**	**30**	**35**
Sec-Butanol	1.0	0.4	0.4	0.4	0.3	0.4	0.9	0.93
MIBK	1.0	0.1	0.0	0.0	0.0	0.0	0.9	0.97
Toluene	1.0	0.3	0.2	0.1	0.1	0.1	0.9	0.95
Butyl Acetate	1.0	0.2	0.1	0.1	0.0	0.1	0.9	0.96
Total Effluent	**1.0**	**0.3**	**0.2**	**0.2**	**0.1**	**0.2**	**0.9**	**0.95**

TABLE D.8
Destruction Data for $\tau = 0.05$ s

(a) Concentration Data (in ppm)

Sampling Time (min)	**0**	**0.5**	**2**	**8**	**15**	**23**	**30**	**35**
Sec-Butanol	34.3	16.4	15.5	16.2	16.5	15.0	31.7	33.9
MIBK	24.1	4.5	3.3	3.0	3.0	2.7	20.3	24.0
Toluene	13.9	5.1	4.5	4.2	3.9	2.1	13.0	14.8
Butyl Acetate	16.0	4.6	4.2	3.9	3.4	2.8	11.9	16.8
Total Effluent	88.3	30.7	27.5	27.2	26.8	22.5	76.9	89.6

(b) Normalized Data (Fraction of Inlet Concentration)

Sampling Time (min)	**0**	**0.5**	**2**	**8**	**15**	**23**	**30**	**35**
Sec-Butanol	1.00	0.48	0.45	0.47	0.48	0.44	0.93	0.99
MIBK	1.00	0.19	0.14	0.12	0.12	0.11	0.84	1.00
Toluene	1.00	0.37	0.33	0.30	0.28	0.15	0.94	1.07
Butyl Acetate	1.00	0.29	0.26	0.24	0.21	0.17	0.74	1.05
Total Effluent	**1.00**	**0.35**	**0.31**	**0.31**	**0.30**	**0.26**	**0.87**	**1.01**

D.3. Destruction Data for Various Applied Voltages

TABLE D.9
Destruction of VOCs vs. Applied Voltage at 300 Hz and $\tau = 0.2$ s

(a) Concentration Data (in ppm)

Applied Voltage (V)	**0**	**9600**	**11400**	**13200**	**15000**
Sec-Butanol	48.2	17.2	16.1	11.2	9.0
MIBK	31.9	3.8	3.4	0.8	0.6
Toluene	9.6	2.0	1.4	1.0	0.6
Butyl Acetate	24.5	3.4	3.3	1.7	1.3
Total Effluent	**117.2**	**26.4**	**24.2**	**14.7**	**3.4**

(b) Normalized Data (Fraction of Inlet Concentration)

Applied Voltage (V)	**0**	**9600**	**11400**	**13200**	**15000**
Sec-Butanol	1.00	0.36	0.33	0.23	0.19
MIBK	1.00	0.12	0.11	0.03	0.02
Toluene	1.00	0.21	0.15	0.10	0.07
Butyl Acetate	1.00	0.14	0.13	0.07	0.05
Total Effluent	**1.00**	**0.21**	**0.19**	**0.11**	**0.09**

D.4. Destruction Data for Humid Runs

TABLE D.10
Destruction of VOCs at 35 – 40 % Relative Humidity, 15 kV, 300 Hz and τ = 0.2 s

(a) Concentration Data (in ppm)

Sampling Time (min)	**0**	**0.5**	**2**	**8**	**15**	**23**	**30**	**35**
Sec-Butanol	31.6	11.9	5.9	2.2	0.9	0.5	27.5	31.5
MIBK	19.9	5.2	2.6	1.3	0.9	0.7	17.8	20.4
Toluene	11.7	3.4	2.1	1.5	1.1	1.1	10.4	12.2
Butyl Acetate	12.3	5.0	3.0	1.7	1.1	0.8	10.3	12.6
Total Effluent	**75.6**	**25.4**	**13.6**	**6.6**	**4.0**	**3.1**	**65.9**	**76.6**

(b) Normalized Data (Fraction of Inlet Concentration)

Sampling Time (min)	**0**	**0.5**	**2**	**8**	**15**	**23**	**30**	**35**
Sec-Butanol	1.00	0.38	0.19	0.07	0.03	0.02	0.87	0.99
MIBK	1.00	0.26	0.13	0.06	0.04	0.03	0.89	1.02
Toluene	1.00	0.29	0.18	0.13	0.10	0.09	0.88	1.04
Butyl Acetate	1.00	0.40	0.25	0.13	0.09	0.07	0.83	1.02
Total Effluent	**1.00**	**0.34**	**0.18**	**0.09**	**0.05**	**0.04**	**0.87**	**1.01**

TABLE D.11
Destruction of VOCs at 70 – 80 % Relative Humidity, 15 kV, 300 Hz and τ = 0.2 s

(a) Concentration Data (in ppm)

Sampling Time (min)	**0**	**0.5**	**2**	**8**	**15**	**23**	**30**	**35**
Sec-Butanol	31.2	7.9	4.0	0.6	0.4	0.4	25.6	29.5
MIBK	22.5	3.2	1.4	0.6	0.2	0.3	18.6	22.1
Toluene	15.2	2.6	1.9	1.3	1.2	1.1	12.4	15.3
Butyl Acetate	14.6	3.2	1.7	1.1	0.4	0.4	11.7	14.1
Total Effluent	**83.3**	**16.9**	**9.1**	**3.6**	**2.3**	**2.1**	**68.3**	**81.0**

(b) Normalized Data (Fraction of Inlet Concentration)

Sampling Time (min)	**0**	**0.5**	**2**	**8**	**15**	**23**	**30**	**35**
Sec-Butanol	1.00	0.25	0.13	0.02	0.01	0.01	0.82	0.95
MIBK	1.00	0.14	0.06	0.03	0.01	0.01	0.83	0.98
Toluene	1.00	0.17	0.13	0.09	0.08	0.07	0.82	1.01
Butyl Acetate	1.00	0.22	0.12	0.07	0.03	0.02	0.80	0.97
Total Effluent	**1.00**	**0.20**	**0.11**	**0.04**	**0.03**	**0.03**	**0.82**	**0.97**

D.5. Destruction Data for Different Reactor Lengths

TABLE D.12
Destruction of VOCs in 2 cm Reactor at 15 kV, 300 Hz and τ = 0.2 s

(a) Concentration Data (in ppm)

Sampling Time (min)	**0**	**0.5**	**2**	**8**	**15**	**23**	**30**	**35**
Sec-Butanol	30.7	4.9	3.2	0.5	0.7	0.6	25.9	31.8
MIBK	21.1	2.6	1.6	0.5	0.4	0.4	17.9	21.2
Toluene	13.4	3.2	2.5	1.5	1.4	1.4	10.9	12.9
Butyl Acetate	14.3	2.6	2.2	1.2	0.8	0.7	11.9	13.9
Total Effluent	**79.6**	**13.3**	**9.4**	**3.8**	**3.2**	**3.1**	**66.7**	**79.9**

(b) Normalized Data (Fraction of Inlet Concentration)

Sampling Time (min)	**0**	**0.5**	**2**	**8**	**15**	**23**	**30**	**35**
Sec-Butanol	1.00	0.16	0.10	0.02	0.02	0.02	0.84	1.04
MIBK	1.00	0.12	0.08	0.03	0.02	0.02	0.85	1.00
Toluene	1.00	0.24	0.19	0.11	0.10	0.10	0.82	0.97
Butyl Acetate	1.00	0.18	0.15	0.08	0.05	0.05	0.83	0.97
Total Effluent	**1.00**	**0.17**	**0.12**	**0.05**	**0.04**	**0.04**	**0.84**	**1.00**

TABLE D.13
Destruction of VOCs in 4 cm Reactor at 15 kV, 300 Hz and τ = 0.2 s

(a) Concentration Data (in ppm)

Sampling Time (min)	**0**	**0.5**	**2**	**8**	**15**	**23**	**30**	**35**
Sec-Butanol	31.3	8.2	2.6	2.5	2.4	2.8	28.4	30.9
MIBK	21.0	1.2	0.6	0.4	0.2	0.2	17.7	20.4
Toluene	13.7	3.5	2.9	1.5	1.3	1.2	10.7	12.8
Butyl Acetate	13.6	1.4	1.0	0.5	0.4	0.4	11.6	13.4
Total Effluent	**79.7**	**14.3**	**7.2**	**4.8**	**4.3**	**4.6**	**68.4**	**77.4**

(b) Normalized Data (Fraction of Inlet Concentration)

Sampling Time (min)	**0**	**0.5**	**2**	**8**	**15**	**23**	**30**	**35**
Sec-Butanol	1.00	0.26	0.08	0.08	0.08	0.09	0.91	0.98
MIBK	1.00	0.06	0.03	0.02	0.01	0.01	0.84	0.97
Toluene	1.00	0.25	0.21	0.11	0.10	0.09	0.78	0.93
Butyl Acetate	1.00	0.10	0.08	0.03	0.03	0.03	0.86	0.99
Total Effluent	**1.00**	**0.18**	**0.09**	**0.06**	**0.05**	**0.06**	**0.86**	**0.97**

TABLE D.14
Destruction of VOCs in 5 cm Reactor at 15 kV, 300 Hz and τ = 0.2 s

(a) Concentration Data (in ppm)

Sampling Time (min)	**0**	**0.5**	**2**	**8**	**15**	**23**	**30**	**35**
Sec-Butanol	36.0	11.0	9.9	7.2	5.2	4.0	35.3	36.9
MIBK	22.3	2.7	1.7	0.8	0.5	0.4	20.5	22.7
Toluene	6.1	1.7	1.5	1.0	0.7	0.5	5.2	6.1
Butyl Acetate	17.2	3.2	2.8	1.5	0.9	0.6	15.1	17.3
Total Effluent	**81.6**	**18.6**	**15.7**	**10.5**	**7.3**	**5.5**	**76.1**	**83.0**

(b) Normalized Data (Fraction of Inlet Concentration)

Sampling Time (min)	**0**	**0.5**	**2**	**8**	**15**	**23**	**30**	**35**
Sec-Butanol	1.00	0.31	0.27	0.20	0.15	0.11	0.98	1.02
MIBK	1.00	0.12	0.07	0.04	0.02	0.02	0.92	1.02
Toluene	1.00	0.27	0.24	0.17	0.11	0.08	0.86	1.01
Butyl Acetate	1.00	0.19	0.16	0.09	0.05	0.04	0.88	1.00
total effluent	**1.00**	**0.23**	**0.19**	**0.13**	**0.09**	**0.07**	**0.93**	**1.02**

TABLE D.15
Destruction of VOCs in 10 cm Reactor at 15 kV, 300 Hz and τ = 0.2 s

(a) Concentration Data (in ppm)

Sampling Time (min)	**0**	**0.5**	**2**	**8**	**15**	**23**	**30**	**35**
Sec-Butanol	37.0	7.9	5.8	4.3	2.8	2.0	31.5	34.6
MIBK	23.9	2.5	1.2	1.3	1.0	0.7	21.1	22.4
Toluene	6.8	2.0	1.1	0.6	0.4	0.3	6.3	6.5
Butyl Acetate	19.6	3.0	2.1	2.0	1.5	1.0	16.4	17.6
total effluent	**87.3**	**15.4**	**10.3**	**8.1**	**5.7**	**4.0**	**75.3**	**81.1**

(b) Normalized Data (Fraction of Inlet Concentration)

Sampling Time (min)	**0**	**0.5**	**2**	**8**	**15**	**23**	**30**	**35**
Sec-Butanol	1.00	0.21	0.16	0.12	0.08	0.05	0.85	0.94
MIBK	1.00	0.11	0.05	0.05	0.04	0.03	0.88	0.94
Toluene	1.00	0.29	0.16	0.09	0.06	0.04	0.92	0.95
Butyl Acetate	1.00	0.15	0.11	0.10	0.07	0.05	0.84	0.90
Total Effluent	**1.00**	**0.18**	**0.12**	**0.09**	**0.07**	**0.05**	**0.86**	**0.93**

D.6. Destruction Data for Multiple Tube Reactors

TABLE D.16
Destruction of VOCs in 10 Tube, 1cm Reactor at 15 kV, 300 Hz and τ = 0.2 s

(a) Concentration Data (in ppm)

Sampling Time (min)	**0**	**0.5**	**2**	**8**	**15**	**23**	**30**	**35**
Sec-Butanol	40.8	3.4	3.0	1.3	0.4	0.3	33.5	37.0
MIBK	26.1	1.3	0.8	0.5	0.4	0.3	21.9	24.4
Toluene	7.7	1.4	1.1	0.7	0.7	0.6	6.4	6.5
Butyl Acetate	21.4	2.0	1.7	1.0	0.7	0.5	17.3	19.7
Total Effluent	**96.0**	**8.1**	**6.5**	**3.5**	**2.2**	**1.8**	**79.0**	**87.6**

(b) Normalized Data (Fraction of Inlet Concentration)

Sampling Time (min)	**0**	**0.5**	**2**	**8**	**15**	**23**	**30**	**35**
Sec-Butanol	1.00	0.08	0.07	0.03	0.01	0.01	0.82	0.90
MIBK	1.00	0.05	0.03	0.02	0.02	0.01	0.84	0.93
Toluene	1.00	0.18	0.14	0.10	0.09	0.08	0.83	0.85
Butyl Acetate	1.00	0.10	0.08	0.04	0.03	0.03	0.81	0.92
Total Effluent	**1.00**	**0.08**	**0.07**	**0.04**	**0.02**	**0.02**	**0.82**	**0.91**

TABLE D.17
Destruction of VOCs in 10 Tube, 5cm Reactor at 15 kV, 300 Hz and τ = 0.2 s

(a) Concentration Data (in ppm)

Sampling Time (min)	**0**	**0.5**	**2**	**8**	**15**	**23**	**30**	**35**
Sec-Butanol	36.3	12.6	12.1	6.9	6.4	6.2	32.6	37.0
MIBK	22.2	2.8	1.8	1.0	0.8	0.6	20.3	23.0
Toluene	5.7	1.9	1.5	0.8	0.8	0.5	5.5	6.3
Butyl Acetate	17.5	3.4	3.0	1.9	1.4	1.0	15.5	18.1
Total Effluent	**81.6**	**20.7**	**18.5**	**10.6**	**9.3**	**8.2**	**73.9**	**84.4**

(b) Normalized Data (Fraction of Inlet Concentration)

Sampling Time (min)	**0**	**0.5**	**2**	**8**	**15**	**23**	**30**	**35**
Sec-Butanol	1.00	0.35	0.33	0.19	0.18	0.17	0.90	1.02
MIBK	1.00	0.13	0.08	0.04	0.04	0.03	0.92	1.04
Toluene	1.00	0.33	0.27	0.14	0.13	0.08	0.97	1.12
Butyl Acetate	1.00	0.20	0.17	0.11	0.08	0.06	0.88	1.03
Total Effluent	**1.00**	**0.25**	**0.23**	**0.13**	**0.11**	**0.10**	**0.91**	**1.03**

APPENDIX E

OZONE EMISSION DATA

E.1. Ozone Concentration vs. Applied Voltage in 1 cm Reactor

This section shows the effluent ozone concentration (in ppm) in dry and humid conditions in the 1 cm reactor. Table E.1 shows effluent ozone concentration in dry air and Table E.2 shows the concentration in humid air. The frequency was maintained constant at 300 Hz and the residence time was 0.2 s for all the runs.

TABLE E.1
Ozone Concentration vs. Applied Voltage in Dry Condition at 300 Hz, and τ = 0.2 s

V''	O_3 (ppm) run1	O_3 (ppm) run2	O_3 (ppm) run3
5734	48.6	48.6	51.0
6617	127.6	136.1	138.8
7500	170.1	156.0	170.1
8559	212.7	221.2	212.7
9619	233.9	233.9	226.9
11385	366.9	382.8	388.9
13151	425.4	397.0	425.4
14916	425.4	425.4	404.1
16682	510.4	510.4	482.1
18448	453.7	425.4	467.9
20214	510.4	467.9	510.4

TABLE E.2
Ozone Concentration vs. Applied Voltage at 35 – 40 % Relative Humidity at 300 Hz, and τ = 0.2 s

V''	O_3 (ppm) run1	O_3 (ppm) run2	O_3 (ppm) run3
6970	97.2	97.2	85.1
8559	141.8	148.9	148.9
11385	191.4	198.5	184.3
13151	212.7	206.6	212.7
14916	234.0	226.9	226.9
16682	255.2	218.8	218.8
18448	255.2	241.1	226.9
20214	212.7	194.5	218.8

E.2. Ozone Concentration vs. Humidity in 1cm Reactor

Table E.3 shows the production of ozone at two different applied voltages (11400V and 18500 V), at different relative humidities. The frequency was maintained at 300 Hz and the residence time for the runs was 0.2 s.

TABLE E.3
Ozone Concentration vs. Relative Humidity at Different Applied Voltages, 300 Hz, and τ = 0.2 s

V''? / ↓% RH	11400 V		18500 V	
	O_3 (ppm) run1	O_3 (ppm) run2	O_3 (ppm) run1	O_3 (ppm) run2
0	366.9	382.8	453.7	467.9
35 – 40	191.4	198.5	241.1	226.9
40 – 50	170.1	170.1	255.2	255.2
50 – 60	136.1	141.8	212.7	198.5
70 – 80	113.4	113.4	170.2	170.2
80 – 90	113.4	106.4	170.2	170.2

E.3. Ozone Concentration in 1 cm and 10 cm Reactors

Effluent ozone concentrations for the 10 cm reactor are shown in Table E.4. The applied voltage was 12.4 kV, frequency was 300 Hz and residence time was 0.2 s.

TABLE E.4

Ozone Concentration (in ppm) in 10 cm Reactor in Dry Condition and 35 – 40 % Relative Humidity at 12.4 kV, 300 Hz, and τ = 0.2 s

Reactor Length	**O_3 (ppm); Dry**			**O_3 (ppm); 35 – 40 % RH**		
	run 1	**run 2**	**run 3**	**run 1**	**run 2**	**run 3**
10 cm	208.8	169.4	205.6	144.5	132.3	176.9

APPENDIX F

ELECTRICAL DATA

The following sections show the electrical data for the different conditions discussed in Chapter 4. For each given condition, the primary and secondary current (I' and I"), primary and secondary power (P' and p''), primary voltage (V'), primary and secondary power factor (pf and pf''), and the wall current (I_w) are tabulated. Table F.1 shows the type of electrical data presented in each section.

Table F.1
Type of Electrical Data Presented in Each Section of Appendix F

Section	Type of Electrical Data
F.1	Electrical Data for Various Reactor Lengths in Dry Condition
F.2	Electrical Data for Various Reactor Lengths in 35 – 40 % Relative Humidity.
F.3	Electrical Data for Different Number of 5 cm Reactors in Parallel

F.1. Electrical Data for Various Reactor Lengths in Dry Condition

TABLE F.2
Electrical Data for 1 cm Reactor at 12.4 kV, 300 Hz and τ = 0.2 s

Run	I" (mA)	pf"	P"	V'	I'	pf	P'	Iw
1	0.241	0.997	2.981	74.385	2.489	0.580	107.391	4.101
2	0.256	0.997	3.185	74.537	2.490	0.580	107.680	4.099
3	0.254	0.992	3.148	74.539	2.490	0.579	107.461	4.106
4	0.254	0.996	3.146	74.231	2.486	0.576	106.311	4.097
5	0.250	0.995	3.092	74.206	2.488	0.580	107.049	4.095

TABLE F.3

Electrical Data for 10 cm Reactor at 12.4 kV, 300 Hz and τ = 0.2 s

Run	I" (mA)	pf"	P"	V'	I'	pf	P'	Iw
1	0.918	0.669	7.621	57.647	1.954	0.598	67.384	3.754
2	0.919	0.670	7.640	57.642	1.953	0.598	67.273	3.758
3	0.919	0.667	7.610	57.637	1.949	0.601	67.510	3.747
4	0.920	0.669	7.645	57.646	1.954	0.598	67.322	3.758
5	0.920	0.670	7.652	57.632	1.949	0.601	67.497	3.751

TABLE F.4

Electrical Data for 20 cm Reactor at 12.4 kV, 300 Hz and τ = 0.2 s

Run	I" (mA)	pf"	P"	V'	I'	pf	P'	Iw
1	1.492	0.615	11.341	44.837	1.520	0.631	43.020	3.777
2	1.556	0.599	11.597	44.003	1.485	0.638	41.706	3.774
3	1.570	0.593	11.504	43.459	1.469	0.631	40.292	3.740
4	1.587	0.590	11.603	43.422	1.470	0.637	40.657	3.738

TABLE F.5

Electrical Data for 30 cm Reactor at 12.4 kV, 300 Hz and τ = 0.2 s

Run	I" (mA)	pf"	P"	V'	I'	pf	P'	Iw
1	2.336	0.529	15.356	36.214	1.166	0.679	28.683	3.810
2	2.431	0.519	15.683	35.505	1.142	0.688	27.892	3.739
3	2.425	0.521	15.612	35.340	1.138	0.684	27.487	3.722
4	2.457	0.518	15.795	35.328	1.127	0.684	27.218	3.722
5	2.485	0.514	15.800	35.009	1.127	0.689	27.160	3.695

TABLE F.6

Electrical Data for 40 cm Reactor at 12.4 kV, 300 Hz and τ = 0.2 s

Run	I" (mA)	pf"	P"	V'	I'	pf	P'	Iw
1	2.989	0.517	19.033	39.557	1.159	0.663	30.387	3.809
2	3.258	0.493	19.886	39.452	1.138	0.660	29.648	3.748
3	3.329	0.491	20.324	39.419	1.136	0.670	29.983	3.763
4	3.321	0.488	20.089	39.190	1.136	0.668	29.727	3.803
5	3.354	0.487	20.282	39.201	1.129	0.662	29.315	3.803

TABLE F.7

Electrical Data for 50 cm Reactor at 12.4 kV, 300 Hz and τ = 0.2 s

Run	I" (mA)	pf"	P"	V'	I'	pf	P'	Iw
1	4.125	0.453	23.084	56.047	1.592	0.613	54.698	3.853
2	4.189	0.450	23.383	56.083	1.589	0.610	54.342	3.831
3	4.218	0.447	23.396	56.088	1.587	0.609	54.188	3.776
4	4.259	0.444	23.473	56.093	1.587	0.612	54.469	3.728
5	4.282	0.443	23.543	56.097	1.586	0.611	54.363	3.737

TABLE F.8
Electrical Data for 60 cm Reactor at 12.4 kV, 300 Hz and τ = 0.2 s

Run	I" (mA)	pf"	P"	V'	I'	pf	P'	Iw
1	5.668	0.403	28.268	74.522	2.139	0.579	92.291	3.473
2	5.608	0.414	28.776	74.610	2.142	0.580	92.759	3.959
3	5.652	0.410	28.704	74.646	2.141	0.580	92.654	3.978
4	5.678	0.408	28.677	74.683	2.138	0.577	92.067	3.976
5	5.699	0.403	28.406	74.705	2.141	0.575	92.013	3.977

F.2. Electrical Data for Various Reactor Lengths in 35 – 40 % Relative Humidity

TABLE F.9
Electrical Data for 1 cm Reactor at 12.4 kV, 300 Hz and τ = 0.2 s

Run	I" (mA)	pf"	P"	V'	I'	pf	P'	Iw
1	0.229	0.998	2.836	74.156	2.487	0.579	106.751	4.086
2	0.232	0.999	2.873	74.191	2.484	0.581	107.167	4.086
3	0.234	0.999	2.893	74.223	2.480	0.580	106.704	4.089
4	0.231	0.998	2.860	74.237	2.483	0.579	106.656	4.100
5	0.228	0.997	2.820	74.207	2.489	0.581	107.229	4.104

TABLE F.10
Electrical Data for 10 cm Reactor at 12.4 kV, 300 Hz and τ = 0.2 s

Run	I" (mA)	pf"	P"	V'	I'	pf	P'	Iw
1	0.881	0.684	7.448	57.526	1.947	0.601	67.301	3.731
2	0.886	0.680	7.450	57.497	1.950	0.600	67.291	3.725
3	0.889	0.682	7.493	57.521	1.942	0.598	66.763	3.720
4	0.891	0.678	7.451	57.487	1.950	0.597	66.879	3.719
5	0.899	0.676	7.525	57.673	1.955	0.599	67.496	3.722

TABLE F.11
Electrical Data for 20 cm Reactor at 12.4 kV, 300 Hz and τ = 0.2 s

Run	I" (mA)	pf"	P"	V'	I'	pf	P'	Iw
1	1.663	0.580	11.933	42.479	1.436	0.636	38.809	3.581
2	1.675	0.575	11.958	42.441	1.444	0.639	39.186	3.598
3	1.680	0.576	12.020	42.457	1.439	0.636	38.862	3.591
4	1.686	0.573	12.010	42.452	1.434	0.639	38.879	3.592
5	1.692	0.575	12.104	42.432	1.438	0.642	39.170	3.596

TABLE F.12

Electrical Data for 30 cm Reactor at 12.4 kV, 300 Hz and τ = 0.2 s

Run	I" (mA)	pf"	P"	V'	I'	pf	P'	Iw
1	2.357	0.521	15.192	35.463	1.132	0.683	27.435	3.714
2	2.454	0.510	15.608	35.084	1.128	0.689	27.279	3.717
3	2.478	0.509	15.742	35.027	1.116	0.689	26.915	3.718
4	2.457	0.513	15.626	34.840	1.115	0.682	26.492	3.701
5	2.485	0.511	15.807	34.795	1.117	0.692	26.882	3.720

TABLE F.13

Electrical Data for 40 cm Reactor at 12.4 kV, 300 Hz and τ = 0.2 s

Run	I" (mA)	pf"	P"	V'	I'	pf	P'	Iw
1	3.175	0.499	19.619	39.803	1.151	0.668	30.622	3.770
2	3.248	0.496	20.059	39.773	1.152	0.670	30.666	3.741
3	3.231	0.496	19.829	39.500	1.148	0.664	30.093	3.714
4	3.243	0.494	19.819	39.492	1.139	0.668	30.059	3.710
5	3.276	0.495	20.104	39.492	1.141	0.660	29.733	3.712

TABLE F.14

Electrical Data for 50 cm Reactor at 12.4 kV, 300 Hz and τ = 0.2 s

Run	I" (mA)	pf"	P"	V'	I'	pf	P'	Iw
1	4.090	0.449	22.811	56.055	1.588	0.611	54.396	3.787
2	4.225	0.446	23.429	56.089	1.597	0.612	54.800	3.681
3	4.178	0.443	22.904	55.787	1.577	0.611	53.808	3.724
4	4.240	0.449	23.573	55.806	1.583	0.608	53.699	3.684
5	4.259	0.441	23.258	55.814	1.577	0.609	53.636	3.732

TABLE F.15

Electrical Data for 60 cm Reactor at 12.4 kV, 300 Hz and τ = 0.2 s

Run	I" (mA)	pf"	P"	V'	I'	pf	P'	Iw
1	5.238	0.457	29.613	73.604	2.119	0.584	91.014	3.876
2	5.396	0.437	29.123	74.042	2.129	0.581	91.569	3.856
3	5.457	0.431	29.102	74.392	2.138	0.579	92.030	3.851
4	5.467	0.433	29.261	74.377	2.143	0.581	92.592	3.824
5	5.631	0.419	29.216	74.703	2.147	0.580	92.979	3.760

F.3. Electrical Data for Different Number of 5 cm Reactors in Parallel

TABLE F.16
Electrical Data for Single 5 cm Reactor at
12.4 kV, 300 Hz and τ = 0.2 s and Dry Condition

Run	I" (mA)	pf"	P"	V'	I'	pf	P'	Iw
1	0.430	0.808	4.308	70.819	2.699	0.642	122.647	4.055
2	0.436	0.799	4.323	70.817	2.704	0.645	123.430	4.046
3	0.437	0.808	4.387	70.833	2.696	0.644	123.060	4.041
4	0.439	0.798	4.350	70.866	2.694	0.639	122.028	4.046
5	0.440	0.798	4.366	70.858	2.704	0.640	122.545	4.045

TABLE F.17
Electrical Data for Four 5 cm Reactors in Parallel at
12.4 kV, 300 Hz and τ = 0.2 s and Dry Condition

Run	I" (mA)	pf"	P"	V'	I'	pf	P'	Iw
1	3.301	0.627	25.679	42.911	1.370	0.809	47.538	3.971
2	3.328	0.623	25.651	42.503	1.357	0.816	47.048	3.956
3	3.359	0.622	25.916	42.494	1.351	0.814	46.743	3.962
4	3.379	0.620	26.050	42.454	1.361	0.813	46.995	3.966
5	3.395	0.616	25.989	42.310	1.355	0.813	46.609	3.950

TABLE F.18
Electrical Data for Six 5 cm Reactors in Parallel at
12.4 kV, 300 Hz and τ = 0.2 s and Dry Condition

Run	I" (mA)	pf"	P"	V'	I'	pf	P'	Iw
1	2.897	0.570	20.538	42.881	1.310	0.693	38.926	3.991
2	2.895	0.564	20.244	42.596	1.309	0.695	38.748	3.990
3	2.904	0.565	20.337	42.637	1.303	0.687	38.177	3.993
4	2.916	0.562	20.341	42.617	1.301	0.696	38.601	3.999
5	2.922	0.561	20.342	42.606	1.307	0.695	38.674	4.003

TABLE F.19
Electrical Data for Eight 5 cm Reactors in Parallel at
12.4 kV, 300 Hz and τ = 0.2 s and Dry Condition

Run	I" (mA)	pf"	P"	V'	I'	pf	P'	Iw
1	3.856	0.566	26.968	58.738	1.683	0.637	63.011	3.963
2	3.906	0.560	27.122	59.225	1.691	0.635	63.598	3.943
3	3.953	0.557	27.399	59.763	1.707	0.635	64.799	3.971
4	3.958	0.557	27.393	59.769	1.706	0.635	64.742	3.967
5	3.966	0.553	27.270	59.800	1.706	0.637	65.007	3.977

TABLE F.20
Electrical Data for Ten 5 cm Reactors in Parallel at
12.4 kV, 300 Hz and τ = 0.2 s and Dry Condition

Run	I" (mA)	pf"	P"	V'	I'	pf	P'	Iw
1	4.387	0.618	33.651	74.952	2.188	0.591	96.928	3.874
2	4.488	0.616	34.267	74.537	2.184	0.587	95.543	3.931
3	4.522	0.617	34.506	74.527	2.188	0.588	95.871	3.924
4	4.622	0.613	35.063	75.045	2.191	0.589	96.781	3.917
5	4.677	0.609	35.182	75.249	2.206	0.589	97.841	3.914

TABLE F.21
Electrical Data for Ten 5 cm Reactors in Parallel at 12.4 kV,
300 Hz and τ = 0.2 s and 35 – 40 % Relative Humidity

Run	I" (mA)	pf"	P"	V'	I'	pf	P'	Iw
1	4.423	0.630	34.373	72.775	2.123	0.589	91.010	3.894
2	4.543	0.619	34.771	73.812	2.163	0.587	93.788	3.904
3	4.562	0.618	34.833	74.013	2.171	0.587	94.237	3.905
4	4.569	0.618	34.832	74.050	2.168	0.585	93.896	3.898
5	4.677	0.612	35.536	75.142	2.200	0.588	97.146	3.921

APPENDIX G

TEMPERATURE PROFILE IN 10 CM REACTOR

G.1. Temperature Profile in 10 cm Reactor

Table G.1 shows the temperature of the effluent gas in the 10 cm reactor at different times after the reactor was switched on. The first row shows the temperature of the gas 2 minutes before the reactor was switched on. The average ambient temperature during the experiment was 62.3 ^{o}F.

TABLE G.1
Temperature of Effluent Gas vs. Time of Run at
Average Ambient Temperature of 62.3 ^{o}F

Time(min)	Reactor temperature (^{o}F)
-2	64.0
0.00	63.2
1.00	63.3
2.50	63.4
3.15	63.6
3.80	64.0
5.00	65.0
6.00	66.0
7.50	67.5
8.50	68.2
9.50	69.2
11.50	70.5
13.34	72.2
16.33	73.7
16.95	74.0
20.10	74.9
21.53	75.2

VITA

Vijay Kalpathi

Candidate for the Degree of

Master of Science

Thesis: DESTRUCTION OF VOLATILE ORGANIC COMPOUNDS IN A DIELECTRIC BARRIER DISCHARGE PLASMA REACTOR

Major Field: Chemical Engineering

Biographical:

Personal Data: Born of May 29th, 1980 in Hyderabad, India. Elder son of K.R. Sundaram and S. Chandra.

Education: Graduated from SRM Jr. College on May 1997; Graduated from Indian Institute of Technology Madras with Bachelor of Technology in May 2002; Completed requirements for Master of Science degree with a major in Chemical Engineering at Oklahoma State University in May 2005.

Experience: Summer Intern in Chandigarh Distillers and Bottlers Ltd, India from April 2001 to July 2001; Employed by Department of Chemical Engineering, Oklahoma State University, as a graduate research assistant; Department of Chemical Engineering, Oklahoma State University, 2002 to present.

Name: Vijay Kalpathi Date of Degree: May, 2005

Institution: Oklahoma State University Location: Stillwater, Oklahoma

Title of Study: DESTRUCTION OF VOLATILE ORGANIC COMPOUNDS IN A DIELECTRIC BARRIER DISCHARGE PLASMA REACTOR

Pages in Study: 95 Candidate for the Degree of Master of Science

Major Field: Chemical Engineering

Scope and Method of Study: The purpose of this study was to optimize the operating conditions for the destruction of VOCs in a dielectric barrier discharge plasma reactor. A representative VOC mixture comprising of s-butanol, toluene, methyl isobutyl ketone and butyl acetate was studied to obtain destruction characteristics. The total concentration of VOCs was initially 100 ppm. The operating parameters studied for optimization were primary voltage (60-110 V AC), frequency (200 – 400 Hz), and relative humidity (0 - 80%). Initial studies were conducted by varying residence time, keeping the other parameters constant, to determine the effect of residence time on destruction efficiency of VOCs.

Findings and Conclusions: The optimum residence time for operation was 0.2 s in the test reactor. A total VOC destruction of 92% was achieved for a primary voltage of 90 V AC (applied voltage across the reactor was 14916 V AC) and frequency of 300 Hz. In general, overall destruction of VOCs increased with an increase in voltage, frequency, and relative humidity. At 90 V primary and 300 Hz, the overall destruction of VOCs was 91% in dry condition and 96% at 35 – 40% relative humidity. The extent of destruction under the dry conditions was in the following order for the four different test molecules: (S-butanol < Toluene < Butyl Acetate < Methyl Isobutyl Ketone). This order changed in humid conditions, suggesting that the destruction mechanism in humid conditions is different due to presence of $OH^{\bullet}$ radicals. Ozone concentration downstream of the reactor increased and stabilized when applied voltage was increased up to 20200 V. With increasing humidity, the ozone concentration downstream was lower. The ozone results showed good agreement with literature observations.

ADVISER'S APPROVAL: Arland H. Johannes